



UNIVERSITY OF  
CAMBRIDGE

Department of Engineering

# Flow of tremie concrete in piles and excavation walls

Author Name: Irina Shmeleva

Supervisor: Dr. Giovanna Biscontin

Date: 28.05.2019

I hereby declare that, except where specifically indicated, the work submitted herein is my own original work.

*Signed* \_\_\_\_\_ *date* \_\_\_\_\_



# **Flow of tremie concrete in piles and excavation walls**

## **Technical abstract**

**Irina Shmeleva, Homerton college**

This project explored the mechanism and causes of formation of mattressing defect, which could occur throughout the process of the bored piles and the excavation walls casting by the Tremie Concrete method. Mattressing is described as a formation of creases through the full thickness of the concrete cover from reinforcement to the concrete surface. The defect could lead to a serious decrease in the durability of the structure due to the exposure of the reinforcement to the aggressive environment, which promotes corrosion. The conditions leading to mattressing are not well researched.

The project hypothesis about the causes of mattressing was formulated based on the results of previous research. It suggested that the mattressing occurs when the high resistance of the support slurry impedes the concrete flow through the reinforcement cage. The aim of the project was to confirm the formulated hypothesis and to determine the combination of concrete and support fluid characteristics, which could lead to mattressing formation.

The series of experiments were conducted to obtain the results supporting the hypothesis. The experiments were carried out using the laboratory set-up, which reproduced the process of tremie concrete placement on a smaller scale. Two types of support slurry (bentonite and polymer) were used throughout the experiments. The variables of the experiment were the values of concrete Slump Flow test and Marsh Funnel viscosity of the support fluid. The values of these variables were within the recommended by literature ranges. The experimental set-up allowed to obtain a video recording of the full process of concrete flow and displacement of the support fluid. Thus, there was an opportunity to reproduce mattressing and to record its gradual development based on the performed experiments. The further experiments, which included a variation of concrete and support fluid parameters, allowed to determine the zone of parameter combinations where the probability of mattressing occurrence is high.

The polymer and bentonite tests with rheometer were performed to assess the influence of rheological parameters of the support fluids on the probability of the formation of mattressing. Shear stress vs shear rate graphs for fluids of different Marsh Funnel viscosities were obtained. The comparison between the recorded slurry characteristics

and experimental results was made. It allowed concluding that the main indicator influencing the mattressing is the shear stress of the support fluid in the range of low shear rate values. For the bentonite slurry described by the Bingham plastic model, this indicator is yield stress. For polymer, the rheometer tests had shown that the shear stress at low shear rates is close to zero. Therefore, the resistance to the polymer slurry flow initiation is minimum and mattressing does not form even at very high values of Marsh Funnel viscosity.

The analysis of differences in the concrete flow patterns for the cases resulting in mattressing and for the cases where mattressing was absent was done based on the video recording processing. The quantitative assessment of the differences in displacements of the vertical and the horizontal components of the concrete flow at the moment of contact with the reinforcement was provided. It was noted that the bentonite slurry with the higher value of yield stress had greater resistance to the horizontal concrete flow through the reinforcement, which could potentially lead to mattressing. This observation was verified by numerical modelling, which qualitatively proved the stated correlation between the slurry yield stress and resistance to the concrete entering the cover zone at the moment of 'enveloping' the reinforcement. Therefore, the formulated hypothesis about the causes of mattressing formation was theoretically and experimentally proved.

Obtained project results revealed the mechanism of mattressing formation during the process of concrete placement by tremie method and could have a practical significance for correcting the recommended material characteristics with account for the identified risk of mattressing.

# Table of Contents

<b>1. Introduction and Literature Review</b>	<b>1</b>
1.1. Tremie method.....	1
1.2. Testing of tremie concrete.....	2
1.3. Research motivation.....	4
<b>2. Formulation of the main hypothesis</b>	<b>7</b>
<b>3. Aim and objectives of the research</b>	<b>9</b>
<b>4. Preparations of the experiment</b>	<b>10</b>
4.1. Experimental set-up.....	10
4.2. Preparation and composition of concrete and support slurry.....	12
4.2.1. Concrete mixture.....	12
4.2.2. Bentonite slurry.....	13
4.2.3. Polymer slurry.....	13
4.3. Experimental Procedure.....	14
4.3.1. Apparatus preparation.....	14
4.3.2. Slurry mixing.....	15
4.3.3. Concrete.....	16
4.3.4. Experiment procedure.....	16
4.3.5. Cleaning-up Procedure.....	17
<b>5. Preliminary Experiment</b>	<b>17</b>
5.1. Slump Flow Test of concrete.....	17
5.2. Results of the experiment and action plan.....	18
5.3. Improvement of experimental set-up.....	19
<b>6. Measurement of Rheological Properties of Support Fluids</b>	<b>21</b>
6.1. Viscometer tests.....	21
6.2. Rheometer tests.....	22
<b>7. Plan and results of experiments</b>	<b>24</b>
7.1. Plan of experiments.....	24
7.2. Results of experiments.....	26
7.2.1. Experiments 1 – 4: bentonite slurry.....	26

7.2.2. Experiment 5: polymer slurry.....	29
<b>8. Discussion</b>	<b>29</b>
8.1. Zone of mattressing formation.....	29
8.2. Comparison of flow patterns.....	32
8.2.1. Bentonite and polymer slurry.....	33
8.2.2. Bentonite slurry: cases where mattressing is and is not present...	34
<b>9. Numerical analysis</b>	<b>38</b>
<b>10. Limitations of the research</b>	<b>45</b>
<b>11. Conclusion and recommendations</b>	<b>46</b>
<b>References</b>	<b>47</b>
<b>Appendix. Risk Assessment Retrospective</b>	<b>49</b>

# 1. Introduction and Literature Review

## 1.1. Tremie Method

The tremie method is a method of casting deep foundations, the elements of which are composed of bored piles and diaphragm walls. The tremie placement method for the “wet method” case is also called slurry displacement method since the concrete flow from the tremie pipe expels the support fluid and fills the drilled hole in the soil. In general, the process of deep foundation construction involves the excavation of soil to form a void space in the ground. Then the reinforcing cage is placed after the excavation completion, and the concrete placement is performed using a tremie pipe. The schematic of preparation and casting of bored piles processes by tremie method is shown in Figure 1.1; the illustrations to the main stages are given in Figure 1.2.

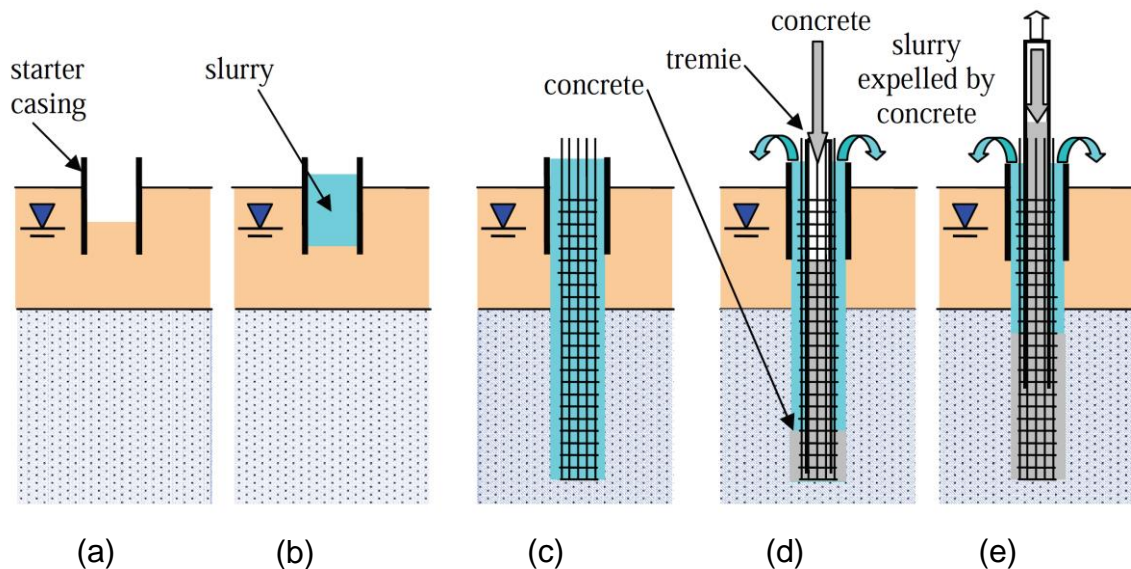


Figure. 1.1. Tremie method schematic:  
(a) set starter casing; (b) fill with slurry; (c) complete and clean excavation, insert reinforcing; (d) place concrete by tremie pipe; (e) raise tremie pipe while pouring concrete (Brown et al, 2010)

In this process the support fluid is required to create backpressure in the borehole during excavation. Seepage must happen in the direction from the excavation into the formation, and not from the formation into the excavation. Inward seepage (into the excavation) is likely to cause sloughing of the sides of the excavation (Drilled Shafts, 2010). Therefore, the slurry prevents the groundwater from entering and maintains the stability of the bored

hole. Support fluids are made from several different types of materials, which are mixed with water. The resulting suspension should have controlled parameters to maintain the stability of excavation walls effectively. Suitable materials include several naturally occurring clay minerals (bentonite) and polymers.

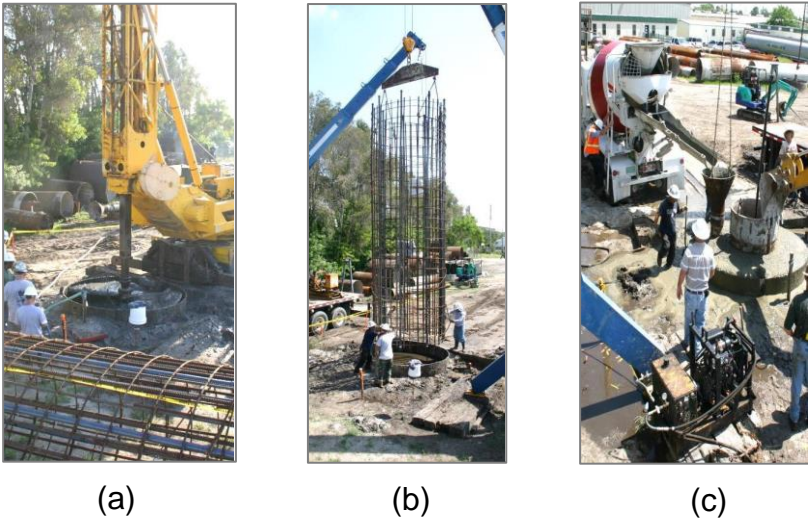


Figure. 1.2. Illustrations for the tremie casting process: (a) excavation; (b) insert reinforcing; (d) place concrete (Bowen, 2013)

The concrete should have sufficient flowability to flow smoothly through the tremie pipe and reinforcement to be used for the tremie method. Together with flowability, tremie concrete should comply with other requirements, which are combined in the general term “workability”. The workability is the ability of the concrete to fill the excavation, self-level and self-compact under gravity (EFFC/DFI, 2018). The workability of the concrete should stay at the required level for the specified duration of time (workability retention). Another key concrete characteristic is stability, i.e. the ability to retain water (filtration and bleed) and resistance to static segregation.

**1.2. Testing of tremie concrete**

The test methods on fresh concrete were developed to ensure that the concrete has a full set of required characteristics. The concrete characteristics are checked on several tests since any single test could not adequately describe all the required parameters. The recommended range and tolerance were developed for each test type.

The main and mandatory test for each tremie concrete delivery batch is the slump flow test (SF). A slump flow test is conducted to quickly check the concrete workability. The

slump flow velocity and the visual stability index test (VSI) are also considered mandatory. Recommended ranges and tolerances for these tests are given in the “Guide to Tremie concrete” (2018) (see Table 1.1).

Test	Recommended Range for Target Value	Tolerance
Slump Flow	400 – 550 mm	± 50 mm
Slump Flow Velocity	10 – 50 mm/s	± 5 mm/s

Table 1.1. Recommended ranges and tolerances for mandatory tests (EFFC/DFI, 2018)

The characteristics of tremie concrete are derived from its rheological properties. The most commonly used rheological model of concrete in a fresh state is the Bingham fluid model with two parameters: yield stress and plastic viscosity (EFFC/DFI, 2018). The relationship between shear stress and shear rate for the Bingham fluid model is given in Figure 1.3.

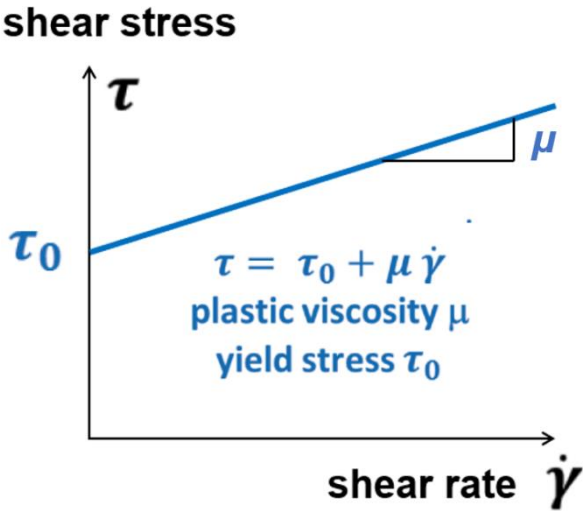


Figure 1.3. Bingham plastic model

Yield stress is the shear stress required to initiate the flow of concrete. Plastic viscosity is the slope of the shear stress vs shear rate line and is a measure of the resistance to flow.

As there are currently no practical field tests to measure these properties directly, indirect measurements are required. Kraenkel and Gehlen (2018) have shown in their research that the slump flow tests can be used to give an indirect measurement of yield stress. Figure 1.4 shows the approximate correlation between yield stress and slump flow.

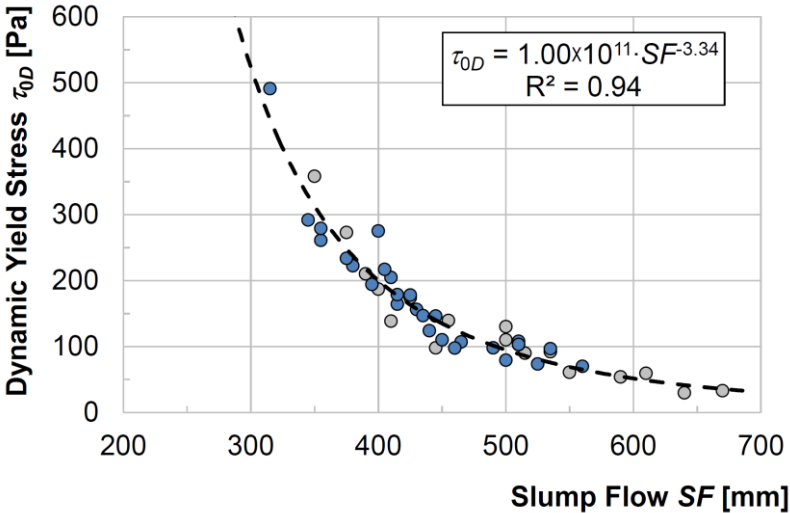


Figure. 1.4. Correlation between yield stress and slump flow (Kraenkel and Gehlen, 2018)

The plastic viscosity could also be obtained from the correlation between slump flow velocity and plastic viscosity, if needed.

**1.3. Research motivation**

Field and laboratory tests are used to study the process of concrete flow when casting deep foundations. Field tests allow to account for in situ factors, but they are the most expensive and time-consuming. Laboratory scale tests could reproduce principal features of the process much faster and cheaper. However, the results of the laboratory tests should be analysed to account for simplifications dictated by laboratory conditions. Nowadays, methods of mathematical modelling of concrete flow is an active area of research. Computer modelling of Tremie Concrete Flow allows investigating the main patterns of the concrete flow at the pouring stage (Roussel et al., 2016; Asirvatham et al., 2017). Moreover, numerical modelling is useful to understand the importance of individual factors influencing the concrete flow and to assess the sensitivity to change in each factor (EFFC/DFI, 2018).

Nevertheless, there are limitations such as high complexity of model preparation, numerical difficulties when modelling the interaction process between liquid and solid bodies and, as of yet, time-consuming calculations when using complex mathematical models. Therefore, the mathematical modelling of tremie concrete flow is mostly used in conjunction with experiments to prove research hypotheses.

Study of the tremie placement process allows to build a robust structure by choosing the correct material parameters and technology. Defects in some cases could be considered as acceptable if they do not affect the bearing capacity or durability. Following classification provided in EFFC/DFI (2018), most imperfections fall into one of the three categories: inclusions, channelling and matting.

Inclusions consist of entrapped material within the foundation that does not conform to the reference concrete. It can be excavated soil, support slurry or poorly cemented material originated from segregated concrete (EFFC/DFI, 2018).

Channelling is a formation of vertical narrow zones on the surface of the casting filled with cement matrix lacking fine aggregates. This phenomenon could cause bleeding of the concrete resulting in cracks and consequently could lead to a reduction in durability (EFFC/DFI, 2018).



Figure. 1.5. Matting defect examples (EFFC/DFI, 2018; Bowen, 2013; Mullins et al, 2005)

Matting is a mismatching on the surface layer of the concrete, which is described as a formation of creases through the full thickness of the concrete cover from reinforcement to the concrete surface (Figure 1.5). Matting could lead to a serious decrease in the durability of the structure by providing access to the reinforcement, which leads to accelerated corrosion of the steel. Therefore, the defect quickly transfers the deterioration process into the final collapse-phase (FIB, 2006). It is worth mentioning that

the defect is hidden (the structure is in the ground) and it cannot be detected with non-destructive testing.

The flow pattern has a significant influence on the possible formation of defects in the cover zone (Bowen, 2013; Lubach, 2010). Flow patterns at concrete pour differ significantly depending on whether reinforcement is present or not. Assumption of a vertical rise of the fresh concrete over the full cross-section of the pile is confirmed only for the case of the unreinforced pile (Fierenkothen and Pulsfort, 2018).

The presence of reinforcement significantly changes the flow pattern (Figure 1.6). Steel bars impede the flow of concrete and cause head differentials from inside to outside of the rebar cage. The difference in the concrete level between the inner and outer portion of the reinforcement cage (head Differential) leads to the appearance of a radial component of the flow (from a reinforced cage into the cover zone).

The reinforcement cage acts as an obstacle to the concrete flow, which provokes the formation of defects in the cover zone between reinforcement and soil surface. There are recommendations to the reinforcement sizing and concrete characteristics (EFFC/DFI, 2018), complying with which lowers the risk of defects. However, the formation mechanism for some defects has not been thoroughly researched, whereas their influence on the durability of the structure could be significant.

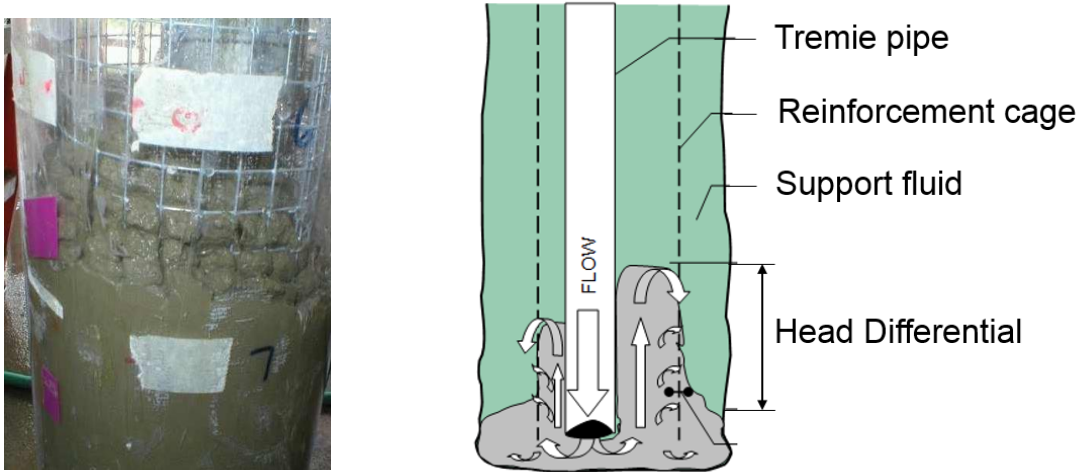


Figure. 1.6. Influence of the reinforcement cage on the flow pattern (EFFC/DFI, 2018; Mullins et al, 2005)

The literature review has shown that there were no reports found in the available publications with detailed research on the causes of the formation of matting.

It is important to research the causes of matting to understand the factors that could lead to the defect. As of now, it is uncertain whether following the existing recommendations for the materials used during tremie concrete placement is enough to avoid matting. It is important to know which concrete and support fluids parameters should be specified and controlled to lower the risk of matting. It would be useful to determine the aspects of concrete and slurry flows promoting the defect. Therefore, the motivation of this research is to obtain results which could help to adjust industry specifications for materials to be used in tremie method and improve the quality of bored piles and diaphragm walls by lowering the risk of matting.

### 2. Formulation of the main hypothesis

South Florida University researchers conducted several experiments reproducing matting defect: they poured specimens with reinforcement by the tremie method (Figure 2.1(a)) (Bowen, 2013).

The influence of the type of the support fluid (polymer/bentonite slurry) and its viscosity on the defect was the focus of the research. It was shown that for the bentonite slurry, which had viscosity higher than a certain threshold, creases in the cover zone were always formed (Figure 2.1(b)). Polymer slurry of the same high viscosity as the bentonite slurry did not produce creases.

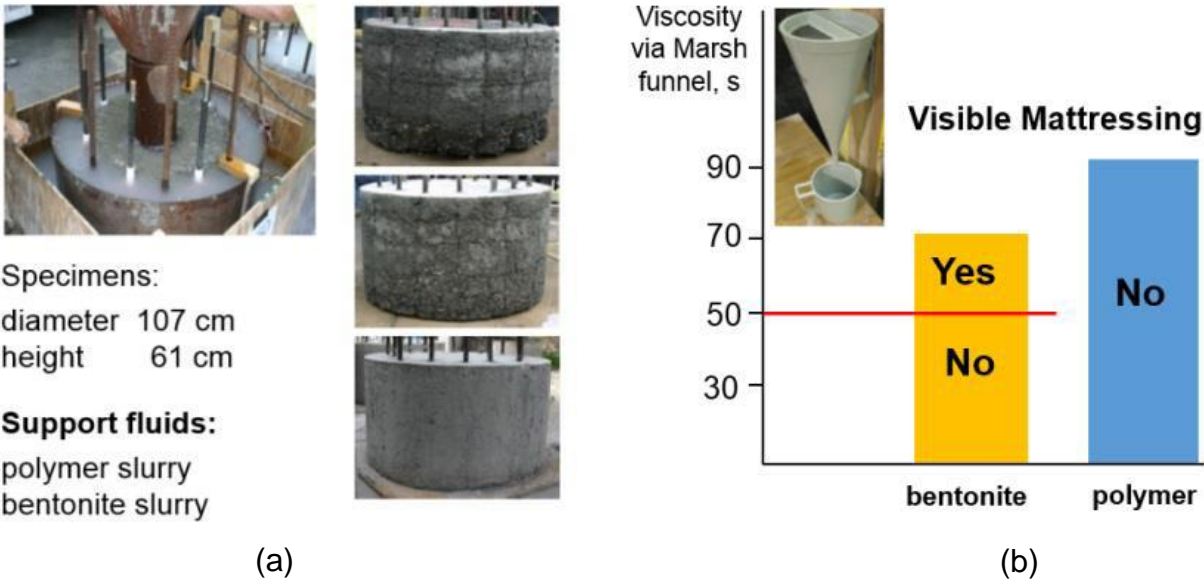


Figure. 2.1. Experiments, where the matting defect was reproduced: (a) Specimens; (b) Results

Therefore, there was an impression that the nature of the support fluid, and not its viscosity, was of the main element with regards to influence on mattressing. Further look into this study has shown that the main variable parameter was assumed to be viscosity via Marsh Funnel (MF). However, the Marsh funnel test is just an indirect measure of the viscosity of the researched fluid. The Marsh funnel viscosity is reported as the number of seconds required for 1000 cm<sup>3</sup> of sample fluid to flow out of a full Marsh funnel (Figure 2.2) and used only as an indicator of the relative consistency of fluids (Brown et al., 2010). True Viscosity, which is a ratio of shear stress to shear rate, is measured by viscometers and rheometers (AMETEK, 2017).

Support fluids belong to a group of non-Newtonian fluids. The Bingham plastic model is used to describe rheological properties of bentonite slurry, and it could also be used for fresh concrete (Figure 1.3). It is important to mention that the range of shear rate values for the support fluid above rising concrete during casting is 0.005-0.01 s<sup>-1</sup> (Lam et al., 2015). Therefore, we are interested in the low shear rate values, which correspond to the shear stress values close to yield stress.



Figure 2.2. Marsh Funnel test (Leutert, 2015)

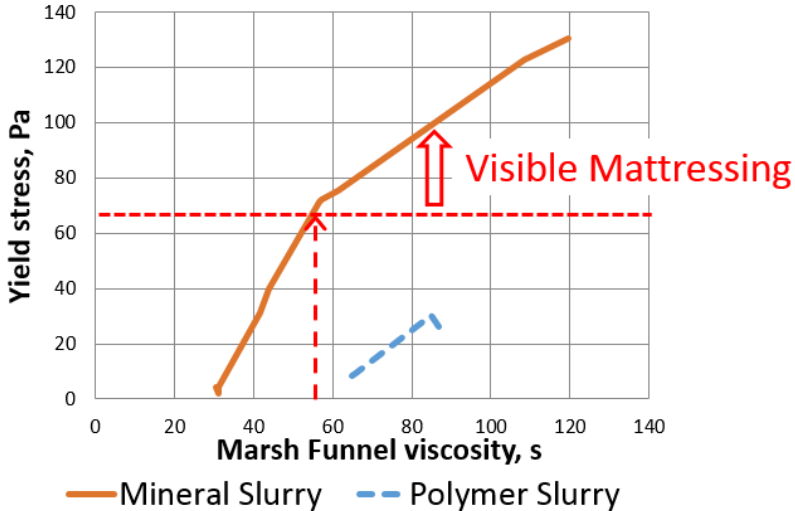


Figure 2.3. Experiment results' interpretation

Bingham fluid parameters were given for reference for the support fluids used in Bowen (2013). These data allowed to plot graphs of yield stress against viscosity via Marsh funnel (Figure. 2.3) for bentonite and polymer slurries. The graphs show that the fluid's yield stress may be a better indicator of mattressing. Below the specific value of yield stress, the defect is not forming either for bentonite or for the polymer slurry.

Therefore, the following hypothesis was adopted: the cause of mattressing is a high resistance of the support slurry to the concrete flow through the reinforcement cage. Slurry resistance to the beginning of flow is primarily determined by the yield stress. Since the concrete characteristics could be varied within the recommended range, it is important to determine a combination of the slurry and concrete characteristics which could lead to mattressing.

### **3. Aim and objectives of the research**

The research aims to verify the hypothesis of the key impact of rheological parameters of the concrete and support fluid on the formation of mattressing.

The following project objectives were defined:

- Determine the combination of bentonite slurry MF and concrete SF, which leads to mattressing. Confirm that the use of polymer slurry even with high MF does not result in mattressing.
- Show that mattressing depends on a support fluid shear stress at a low shear rate and that this correlation is true for bentonite slurry and polymer slurry.
- Determine the differences in flow patterns between the cases resulting in mattressing and those where mattressing was absent and explain the reasoning behind those differences.

The following main steps were planned:

1. Prepare and run the trial experiment with the experimental setup, which reproduced the process of tremie concrete placement on a smaller scale. Video record the full process of concrete flow and displacement of the support fluid.
2. Based on the experimental results, if needed, improve the experimental setup and experiment methodology.
3. Obtain visible mattressing defect by varying the parameters of the bentonite slurry and concrete. The combination of support fluid and concrete parameters at which visible mattressing is obtained first will be taken as a starting point (Figure 3.1).

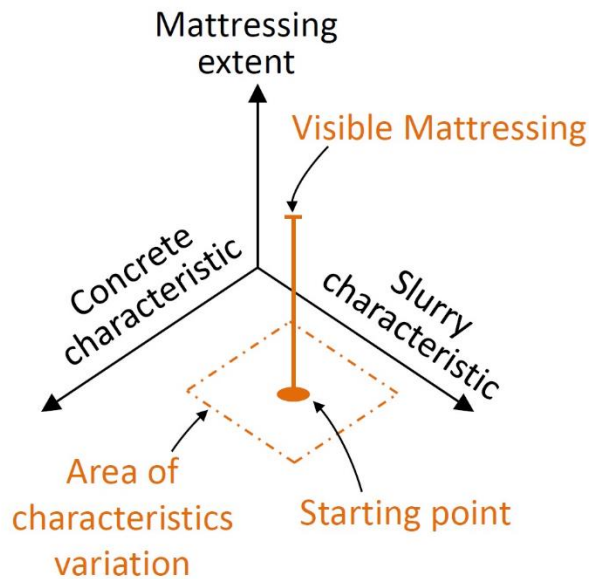


Figure 3.1. Concept of the experiment

4. Run a series of experiments around the starting point. This will allow assessing the sensitivity of the response (the extent of mattressing) to changes in the parameters (the bentonite slurry MF and concrete SF).
5. Complement the first series of experiments with bentonite slurry with a second series of the experiments with polymer slurry of high MF viscosity.
6. Measure the rheological properties of the support fluids. Obtain the relationship between shear stress vs shear rate (including low shear rate values) for bentonite and polymer slurries of different MF values.
7. Compare experimental results and the values of rheological properties of the support fluids used in the experiments. Analyse the relationship between rheological properties and the extent of mattressing.

## 4. Preparations for the experiment

### 4.1. Experimental set-up

The project aims and objectives required to develop an appropriate experimental set-up for the tremie concrete testing series. It was decided to use experimental set-up designed and built last year, which was also used for tremie concrete experiments (Buglass, 2018). It is a 1:6 scale model of the typical pile used in the industry. The dimensions of such pile were taken from the EFFC/DFI Guide (2018) and scaled accordingly for the set-up. The

main parts include: the gravity flow box, hopper, tremie pipe, pulley and support frame (Figure 4.1). Since the experiment involves operations with the support fluid, the initial modification to the set-up was attaching side pipe with a small funnel at its end to avoid spillage when pouring the support fluid inside the box.

The gravity flow box is a transparent Perspex box of overall dimensions 50x200x1000 mm. Its faces are connected with M4 bolts spaced at 65 mm on centre with a rubber strip glued to the edges to protect against support fluid/concrete leaks. The box is bolted to a 300x300 mm PVC bottom plate which also has glued rubber strips on the four edges.

The hopper is a 10 L modified plastic container which is connected to a pulley by ropes at its sides. The hopper is attached to 1 m PVC tremie pipe by means of the hopper-tremie pipe connection. The tremie pipe diameter is 40 mm. The vertical stability of the pipe-hopper system preventing rotation is provided by a support frame. The overall stability of the experimental set-up is provided by 350x350x2900 steel support frame. The pulley system is fastened to the support frame as well.

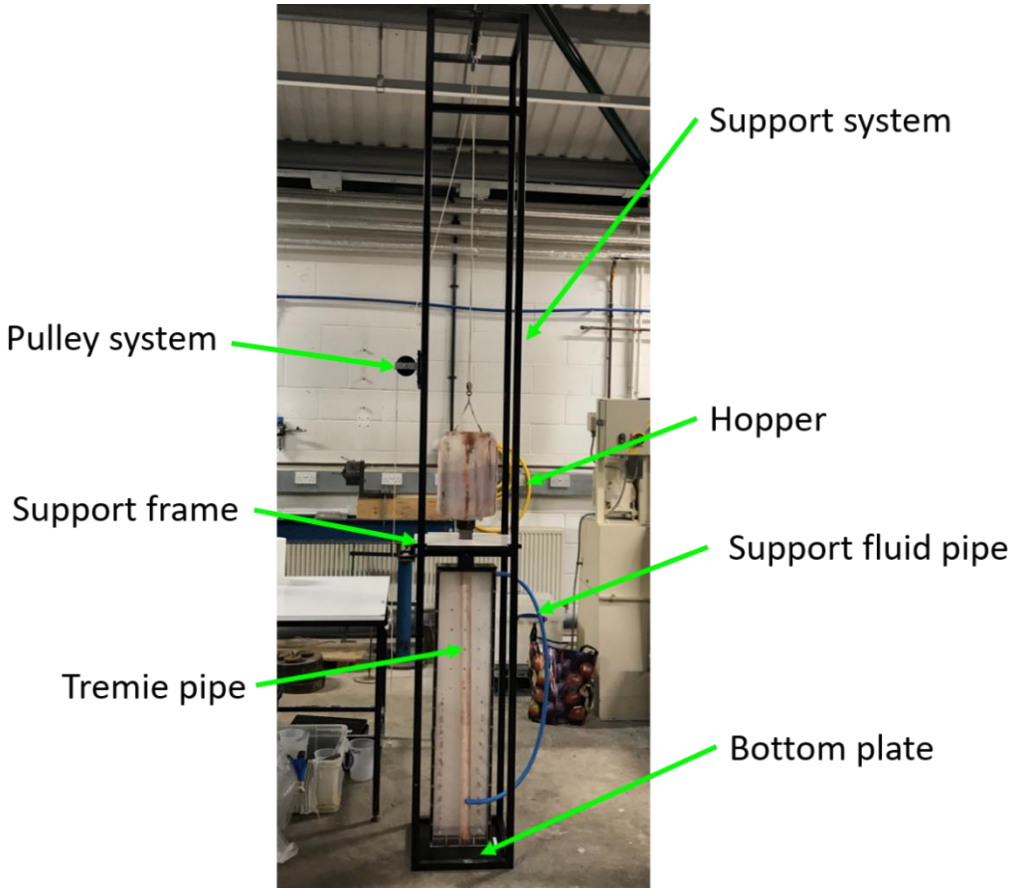


Figure 4.1. Main parts of the Experimental Set-up

## 4.2. Preparation and composition of concrete and support slurry

### 4.2.1. Concrete mixture

A unique concrete composition needed to be developed for the experiments in the scaled experimental set-up. The tremie concrete mix used in industry (EFFC/DFI, 2018) could not be used during the tests since maximum aggregate size is 20 mm while the experimental tremie pipe diameter is just 40 mm which limits the maximum aggregate size to 7 mm (since the minimum pipe diameter should be 6 times bigger than the size of maximum aggregate). Therefore, it was decided to use the mix designed by Fierenkothen and Pulsfort (2017) for experiments on a pile of length 1 m. This mix was also used in last year experiments on tremie concrete in the same set-up since the concrete flowed acceptably according to results (Buglass, 2018). Table 4.1 shows the products used in tremie concrete mixture and Table 4.2 shows concrete mixture composition for a 16 kg batch, which was the amount required to perform both a SF test and an experiment.

The aims of the experiment required to use the concrete mix of different SF result. According to the EFFC/DFI Guide (2018), a more stable concrete mix (i.e. the one with the lower SF diameter) could be obtained by varying the water-cement (w/c) ratio. As it will be shown later, the SF result for concrete of composition from Table 4.2 is 550 mm with the w/c ratio of 0.55. To get the mix of lower w/c the mass of cement was increased accordingly.

Material	Producer	Product/Grade
Water Cement + Fly Ash	CEMEX	CEM II/B-V 0.15 - 0.30 mm: 3402 0.40 - 1.40 mm: 3407
Sands / Aggregates	Specialist Aggregates	1.00 - 2.00 mm: 3409 2.00 - 3.00 mm: 2639F 3.00 - 5.00 mm: 2640 5.00 - 8.00 mm: 2641
Superplasticiser	BASF	SKY 920

Table 4.1. Products used in tremie concrete mixture

Material	Mass per 16 kg batch / g
Water	1700
Cement + Fly Ash	3100
	0.15 - 0.30 mm: 3402
	0.40 - 1.40 mm: 3407
Sands / Aggregates	1.00 - 2.00 mm: 3409
	2.00 - 3.00 mm: 2639F
	3.00 - 5.00 mm: 2640
	5.00 - 8.00 mm: 2641
Superplasticiser	13

Table 4.2. Concrete mixture composition for 16 kg batch

#### 4.2.2. Bentonite slurry

Bentonite slurry is prepared by mixing dry sodium bentonite powder and water with a Stuart SS10 Stirrer. The bentonite used in the experiments is produced by Fisher Scientific UK Ltd. The test performed on the slurry before the experiment is MF test. The target level of MF viscosity for the first experiment (upper bound of the recommended range) was approximately 50 s. It is known from previous studies (Bowen, 2013) that this is consistent with adding bentonite into the water in the following proportion: 0.95 lb/gal = 114 gram /cubic decimeter. In the later tests, bentonite of lower MF viscosity was required, and it was achieved by varying the bentonite content accordingly.

#### 4.2.3. Polymer slurry

The preparation procedure for the polymer slurry is different from that of bentonite slurry. It was decided to use Enhanced Slurry Pro by KB International. It is the same mixture that was used in the Lam et al. (2014) research where the properties of polymer slurry were studied. The ingredients and their concentration were taken from Damji (2018). The concentration required for use in clayey soil was chosen for the experiment since the performance criteria of the polymer slurry depending on the soil was not the focus of this research. The polymer mix comprises the pure polymer powder, (SlurryPro CDP) along with two additives. The water for the slurry was treated to a pH of 10.5 to comply with

industry standards (Lam and Jefferis, 2017). The concentration of the components for 4 L mixture is shown in Table 4.3. Harsh mixing could cause the polymer chains to tear apart; thus, the solution should be gently mixed by air bubbles from a perforated plastic tube connected to the laboratory air supply at pressures below 20 kPa. The mixing should continue for 45-60 minutes, and the solution should be left overnight to ensure a complete reaction with water.

Chemical component	Concentration in clayey soils/ kg/m <sup>3</sup>	Mass per 4 L batch/ g
Slurry Pro CDP	1.1250	4.50
Enhance it 100	0.0750	0.30
Enhance it 200	0.0275	0.11

Table 4.3. Polymer slurry composition for 4 L batch

### 4.3. Experimental procedure

#### 4.3.1. Apparatus preparation

The apparatus should be prepared before each experiment. Firstly, the front side of the gravity flow box is disassembled, and reinforcement installed. The reinforcement is made of 48 mm length and 7 mm diameter wooden sticks glued to the back and the front side of the box with glue dots at 50 mm spacing. This agrees with industry guidance on reinforcement spacing: 4 x diameter of reinforcement (EFFC/DFI, 2018). A nominal concrete cover of at least 75 mm is recommended for industry use, thus, considering a 1:6 scale, the chosen concrete cover of 25 mm is sufficient for the experiment. The reinforcement sticks were positioned as shown on Figure 4.2 (a): one at each side in 10 rows.

The next step is to install rectangular foam laying at the bottom plate of the box (Figure 4.2 (b)) to protect against concrete/support fluid leaks. Then the foam at the end of the tremie pipe (Figure 4.2 (c)) was attached to avoid the support fluid coming inside the tremie pipe while the concrete is loaded into the hopper.

Finally, after the apparatus was prepared, the camera was positioned in front of the box at the height of approximately 300 mm and at the distance of 0.5 m from the box to get

a view of all reinforcement layers. A black card was placed on the floor between the camera and the box to reduce reflections affecting the quality of the video.

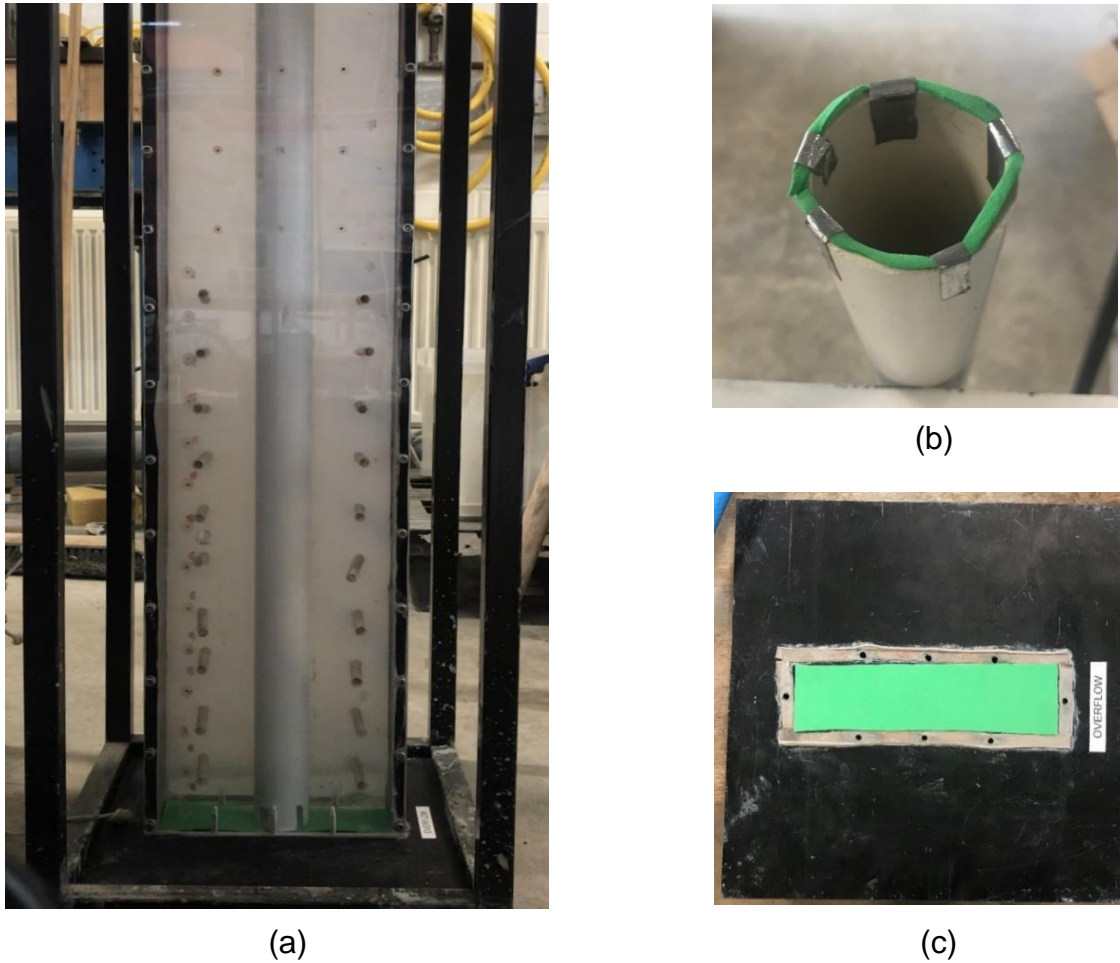


Figure 4.2. (a) Reinforcement layout; (b) bottom plate laying; (c) tremie pipe laying

#### 4.3.2. Slurry mixing

Bentonite slurry was prepared after assembling the apparatus. Approximately 1.5 L of the mix was prepared for each experiment. The required mass of bentonite powder was measured on a scale with an accuracy of 0.01 g. High precision of measurement is necessary because the relationship between Bentonite Mix Ratio and MF Time is highly non-linear and, therefore, the mass of bentonite in a mix should be carefully controlled. After measuring the mass of bentonite and water, a stirrer paddle was inserted into the container with water and the stirrer was set to around 300 RPM. The 20 g of bentonite powder was then added, RPM increased to 1000 and the mixture left for 20 minutes. This step was repeated until all the bentonite was mixed into a slurry. After that, the slurry was left to thoroughly mix for around 3 hours at 1500 RPM.

The procedure for mixing polymer slurry starts with weighing components on the same scale as bentonite. Then the perforated plastic tube connected to the laboratory air supply is inserted into the bucket with water. The polymer is then slowly added to the water by around five granules at a time. It is then gently mixed with a wooden paddle. Care was taken to minimise the amount of polymer getting attached to the walls of the container. Then the additives were sprinkled and carefully mixed. The resulting slurry was left mixing with air bubbles for around 60 minutes. It was then left to rest overnight before using in the experiment.

MF test was then performed on the mixed slurry. The slurry was poured into the funnel through the metal grid (to get rid of air bubbles and undissolved bentonite/polymer) and the time (in seconds) taken to fill the container was recorded. The bentonite slurry was mixed to either 50 s (155.08 g of bentonite per 1500 g of water) or 35 s (85.35 g of bentonite per 1500 g of water). The polymer was mixed to 81 s (see Table 4.3 for details of ingredients). The bentonite slurry was then tested on a Brookfield viscometer.

#### **4.3.3. Concrete**

Concrete is prepared simultaneously with slurry. The grades of sands and aggregates, water and superplasticiser were measured with 0.1 g accuracy. Each batch was weighed to within 10 g to improve the reliability and accuracy of the results. According to Laing O'Rourke guidance on mixing procedures, all sand and aggregates were mixed with 50 % of water required for the total mix in a bucket. Then the bucket was covered with plastic sheeting and left for 30 minutes to saturate. After that, the cover was removed, and the cement added. Care was taken to limit the production of dust. The remaining water with superplasticiser mixed in was then added to the mixture in 200 – 300 ml intervals. The concrete was mixed thoroughly with a handheld mixer to achieve uniform consistency and minimise the possibility of segregation. The Slump Flow Test, in accordance with BS EN 12350-2:2009 was performed afterwards.

#### **4.3.4 Experiment procedure**

The experiment was ready to be performed after the support fluid and concrete were prepared. The process required two people. The first person poured the bentonite/polymer slurry into the box through support fluid pipe; the second person held the tremie pipe tight against the base plate to avoid slurry flowing into the tremie pipe.

Then, the concrete was loaded into the hopper. After that, the person holding the tremie pipe raised it by approximately 30 mm using the rope pulley system, so that the concrete could flow out displacing the support fluid. The experiment stopped when all the concrete was poured inside the box. The whole duration of the experiment was recorded by a video camera.

#### **4.3.5 Cleaning-up Procedure**

Cleaning-up commenced after the video of the experiment was recorded, and all the additional photos/measurements were taken. Firstly, the tremie pipe and hopper were taken off the apparatus, then the gravity flow box was dismounted from the support frame and the leftover concrete and support fluid were wiped off with damp paper towels. The reinforcement sticks were collected and cleaned to be used in the next experiment. The foam and glue sticks were detached from surfaces and disposed of in an environmentally responsible way since they were single use only. The concrete was disposed of using the lab skips.

### **5. Preliminary experiment**

The aim of the preliminary experiment (or experiment 0) was to assess the potential of obtaining the mattressing defect. It was also a chance to master the testing equipment, to find possible areas of improvements to experimental procedure/set-up and to determine the next steps of the research. Only bentonite slurry of the upper bound of the recommended range (which is 50 s Marsh Funnel viscosity) was used at this stage since its use in earlier experiments had led to defects forming. Concrete of the upper bound of the recommended range of SF Test results (550 mm) was prepared.

#### **5.1. Slump Flow Test of concrete**

As it was mentioned before, the SF test was conducted before the experiment. It was done to ensure that the tremie concrete was at the upper bound of the recommended industry range. The British Standard procedure was strictly followed. Two orthogonal slump's diameters were measured as 550 mm and 570 mm. This was done using a measuring tape with accuracy of 10 mm. Based on Figure 5.1, it could be concluded that the concrete mixture showed signs of bleeding. This bleeding was considered

insignificant for the experiment; hence, the mixture consistency was accepted as satisfactory.



(a)



(b)

Figure 5.1. (a) Concrete in a bucket; (b) Concrete SF Test result

## 5.2. Results of the experiment and action plan

On the day of the experiment, slurry was mixed to 50 s MF viscosity and concrete to 550 mm SF. After filling approximately half of the box with the support fluid, the concrete mixture was loaded into the hopper. Then the pipe raised by about 30 mm for the concrete to escape. However, the flow of the concrete out of the pipe was insignificant even after application of considerable vibrations to the hopper. The volume of the escaped concrete was insufficient to reach the reinforcement (Figure 5.2 (a)).

In comparison with last year experiments, when the same set-up and concrete mix were used (just without the support fluid), there were considerable difficulties of flowing concrete through the pipe in this experiment. Only a small portion of the concrete came out of the pipe. After disassembling the box, the mixture presented in Figure 5.2 (b) was found. It was a jelly-like consistency mix, which was the result of the concrete and support fluid interaction. This was an interesting result to obtain since the same mixture is formed at the support fluid-concrete interface when the real pile is cast, and it could potentially be a subject for further research.

Several blockages prevented the flow of concrete: in the pipe itself (potentially due to old concrete on the inner surface of the tremie pipe) and at the bottleneck section (since the

cross-sectional area of the hopper hole is 20% less than that of the pipe). The connection between the hopper and pipe should have had a minimum diameter of 40 mm for the maximum aggregate size of 7 mm. However, the actual diameter of the hopper neck was just 36 mm. The problem was complicated even more by the fact that some aggregates were of size 8 mm. Initially it was assumed that the difference of just 1 mm would not cause difficulties in flow, however, in practice, this assumption turned out to be incorrect. Therefore, there was a clear need to improve the experimental set-up and repeat the experiment with the same characteristics of concrete and support fluid. As it was mentioned earlier, the main problem was blockages in several places. Hence, a new pipe was installed, and the tremie pipe-hopper connection changed to avoid reductions in diameter. There was also a big hydrostatic pressure produced by the support fluid, so it was hard for the concrete to flow out by gravity. In the next experiment, a maximum of 30 cm of support fluid height was used to lower the pressure.

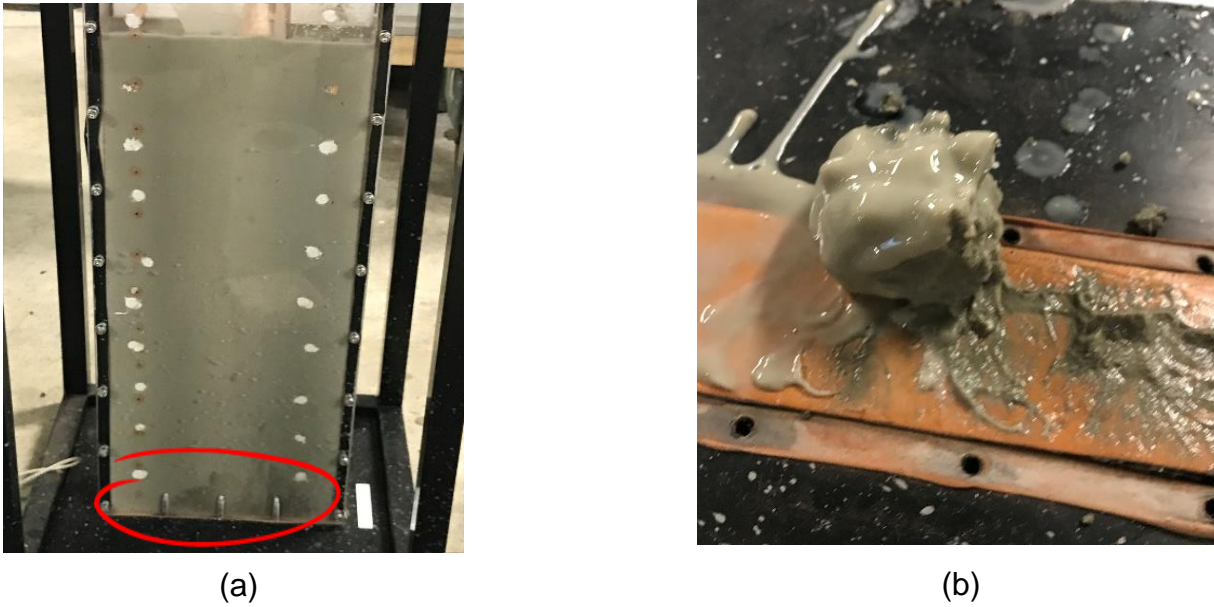


Figure 5.2. (a) Difficulties of flowing concrete through the pipe;  
(b) Result of the concrete and support fluid interaction

### 5.3. Improvement of the experimental set-up

The focus of the improvement of the experimental set-up was the re-design of the tremie pipe-hopper connection. Figure 5.3(a) shows new plastic parts: these were grooved where required and then assembled to form a connection shown in Figure 5.3(b). A hopper of bigger bottleneck diameter was used as well. It can be seen that the new

arrangement of the connection between pipe and hopper is different from the previous one: this time the pipe is inserted into the hopper. The overall diameter of the connection is thus limited to the internal diameter of the pipe, which is 43.5 mm. Therefore, the aggregates of size 7 mm could now be used in the concrete mix according to the guidance in (EFFC/DFI, 2018). However, to stay on a safe side, the 6.4 mm sieve was used in all the following experiments to limit the maximum size of aggregates and thus prevent the possibility of blockage.

The new connection was designed with the idea that the pipe can be changed to a new one for each experiment since the concrete residue on the inside surface of the pipe was a problem in the preliminary experiment. Therefore, the connection should be easily disassembled, and the pipe replaced. Another advantage of such a set-up is the ability to thoroughly clean the inside surfaces of the connection after each experiment.

As will be discussed later, the new set-up proved to be effective. There were no problems with concrete flowing through the apparatus and blockages were not formed. The connection was disassembled and cleaned each time. Although the pipe was cleaned after each experiment, aggregates in the concrete left scratches on the internal surfaces, thus limiting the use of a pipe to a maximum of 2 times.

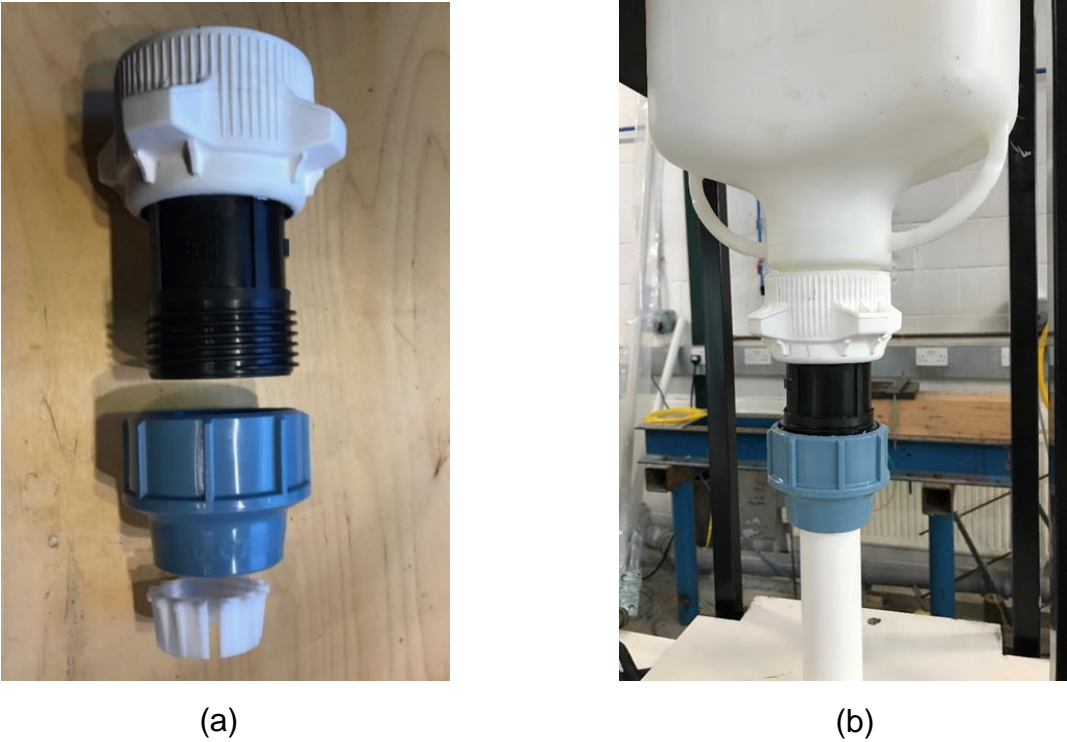


Figure 5.3. (a) New plastic parts for the improved hopper-pipe connection  
(b) Improved connection

## 6. Measurements of Rheological Properties of Support Fluids

As it was shown before, the rheological parameters of the support fluid could have a significant impact on the risk of matting. In that regard, this project pays particular attention to the study of support fluid characteristics.

### 6.1. Viscometer tests

By using the Brookfield DV-E Viscometer, the viscosity parameters and spring torque for bentonite slurry used in the experiment were measured (Marsh Funnel viscosity of the fluid was 51 s) (Figure 6.1). The graphs were plotted based on the average values from several measurements. It should be noted that there was a significant scatter of the viscosity and torque values (up to 50% deviation) for the same RPM for the area of low RPM values (up to 20 RPM). At higher RPM, the data reliability increased significantly. For bentonite slurry, we are particularly interested in yield stress which is associated with the Bingham plastic model. It is pointed out in the literature that the yield stress depends on the measuring and analysis method used (Barnes, 1985). The method of determining dynamic yield value is given in the manual of the Brookfield Viscometers (AMETEK, 2017). This method involves plotting viscometer torque readings versus speed (RPM). The line thus obtained is extrapolated to zero RPM (using a “best fit” line – see the dotted line in Figure 6.1(b)).

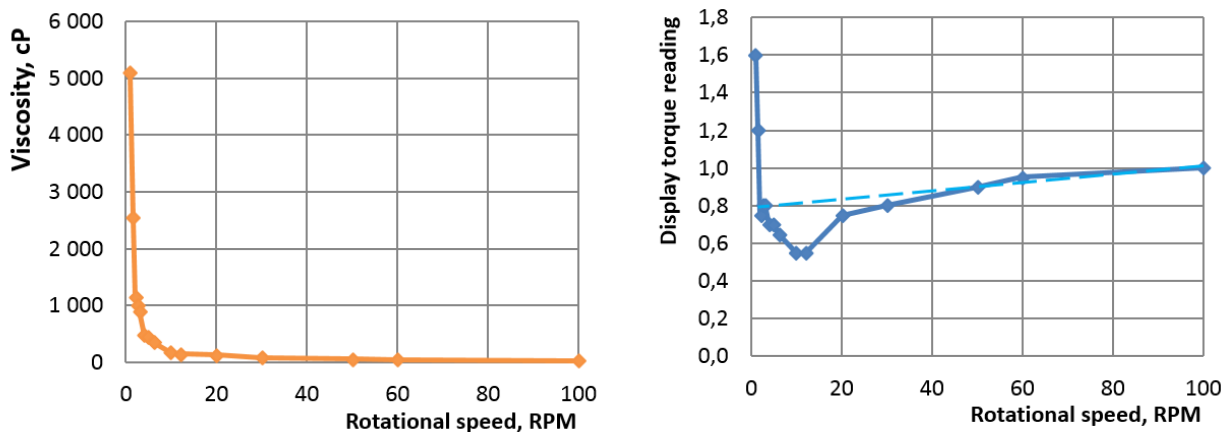


Figure 6.1. Viscometer measurements results: (a) Viscosity; (b) Torque

The corresponding value for the viscometer torque reading represents the dynamic yield value. The coefficient, which depends on the viscometer model and the type of spindle, is used to convert torque values to shear stress values.

The accuracy of the shear stress results should be higher than the accuracy of the Viscometer for the aims of this research. Large scatter of results at the initial segment of the graph, and the following extrapolation of results do not allow to carry out a valid comparison of yield stress for the support fluids used in the experiments. Therefore, the main measurements of rheological properties of support fluids were undertaken by rheometer.

**6.2. Rheometer tests**

After the initial investigations with the Brookfield DV-E Viscometer, further rheological tests were carried out to characterize the flow behaviour of the support fluids over a broader range of shear rates, particularly lower shear rates.

Kinexus Rheometer was used for testing support fluids. The model Kinexus-pro has a torque range from 10 nNm to 200 mNm, so it enables measurements to be made at very low shear rates. The torque resolution is 0.1 nNm and the angular position (strain) resolution is 10 nano-radians.

Density and MF viscosity values of the fluids that were tested are given in Figure 6.1.

	Bentonite fluid		Polymer fluid	
Density, kg/m <sup>3</sup>	1035	1075	874	907
Marsh Funnel viscosity, s	35	49	81	159

Table 6.1. Parameters of the fluids tested by rheometer

Measurements of rheological parameters were taken several times for each support fluid to confirm the repeatability of the results. The examples of “shear stress versus shear rate” graphs for the three tests of polymer slurry with MF of 81 s and two tests of polymer slurry with MF of 159 s are shown in Figure 6.2.

“Shear Stress vs Shear Rate” graphs for fluids used in further experiments are given in Figure 6.3. The same graphs for bentonite slurry at the low shear rate values (from 0 to 1 s<sup>-1</sup>) are presented in Figure 6.4. Results show that the bentonite slurry indeed behaves according to the Bingham plastic model. Therefore, the yield stress of bentonite slurries could be determined: 1.1 Pa and 7.7 Pa for the slurry with 35 s MF and 49 s MF respectively.

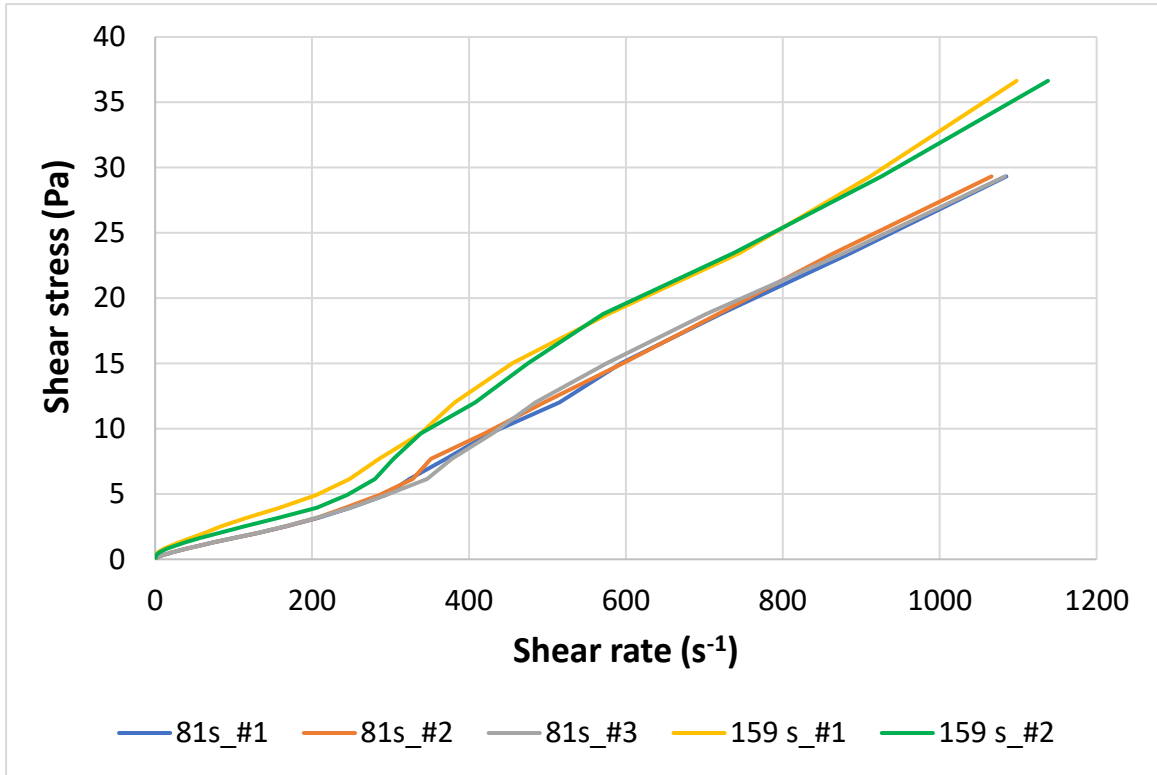


Figure 6.2. Tests of polymer fluids

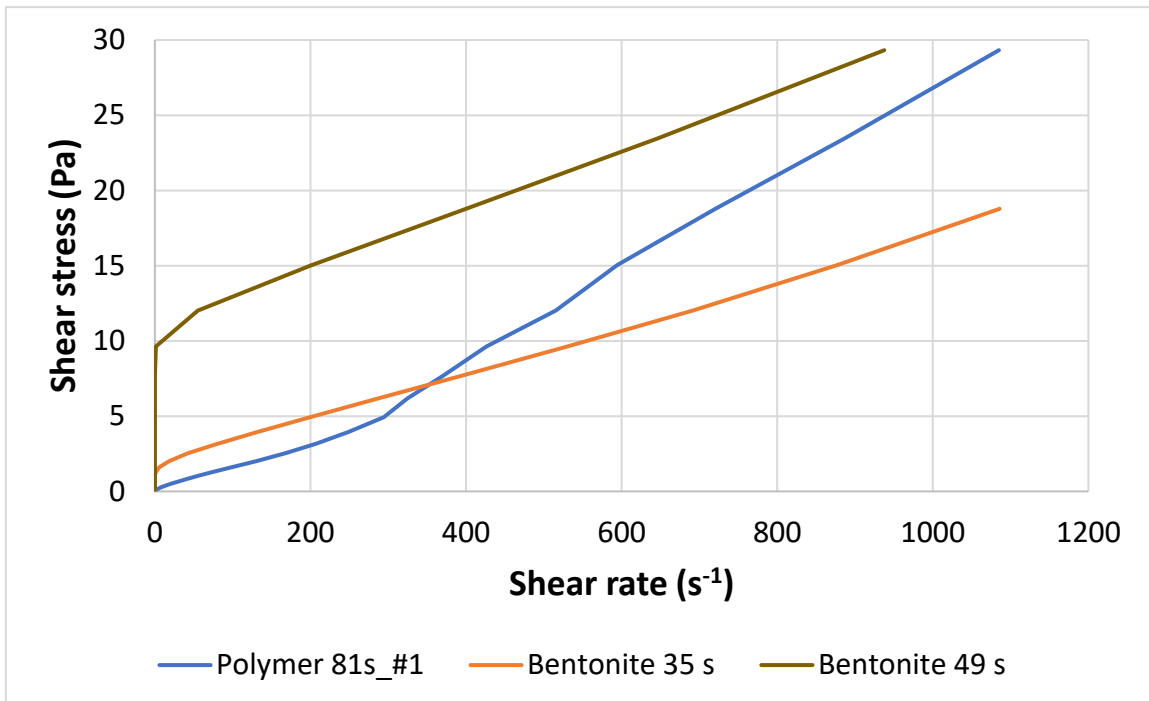


Figure 6.3. Rheometer test results for polymer and bentonite slurry

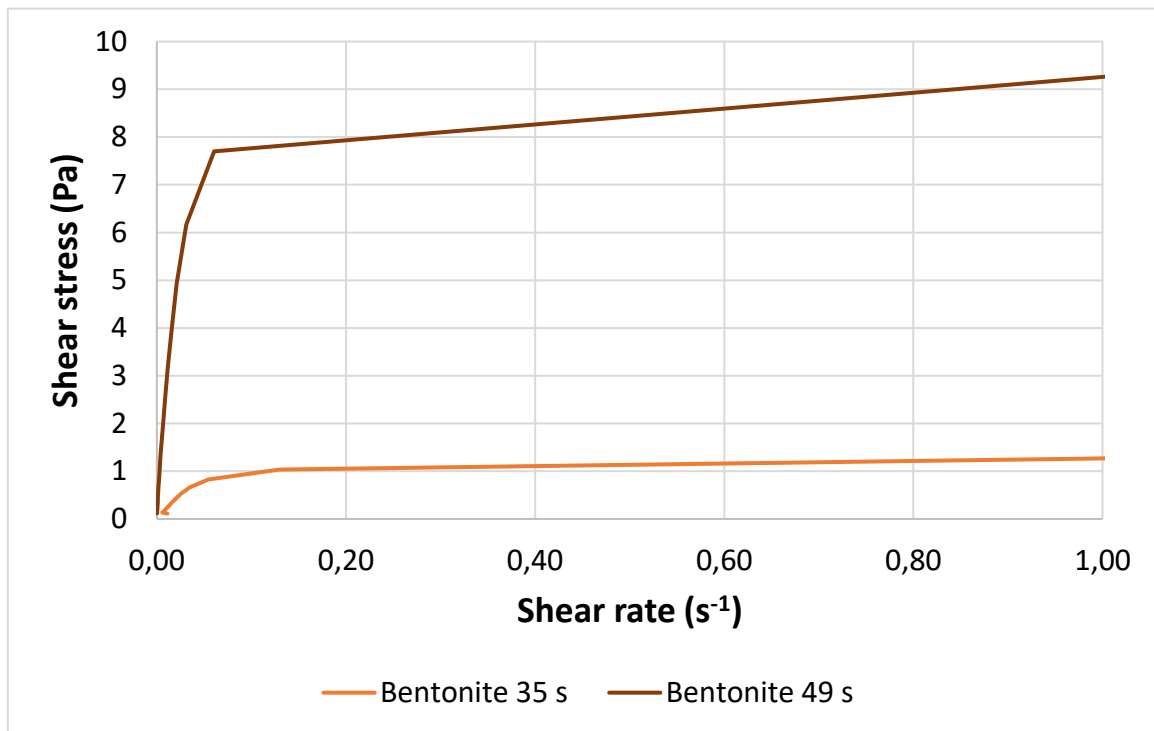


Figure 6.4. Shear Stress vs Shear Rate for bentonite slurry at low shear rate values

The shape of the graph for polymer slurry does not agree with the Bingham model. Shear stress graphs for polymer slurries start nearly at zero, and this feature does not depend on MF result. There is no initial graph segment, which could be associated with non-zero yield stress. It proves that the shear stress required to initiate the flow of polymer slurry is close to zero.

## 7. Plan and results of experiments

### 7.1. Plan of experiments

A plan for the experimental program was developed according to the concept shown in Figure 3.1.

The variables under consideration were the values of the concrete SF and MF of the support fluid. The result to be evaluated was the extent of mattressing.

The first experiments aimed to find a combination of support fluid and concrete parameters at which the visible mattressing would be present. First three experiments were conducted with the bentonite slurry of constant MF at the upper bound of the recommended range (see Figure 7.1). The SF of concrete was changed according to the following scheme: the maximum value of the recommended range → minimum value of

the recommended range → intermediate value defined based on the results of the first two experiments.

Two more experiments were conducted after obtaining the mattressing effect. This time the SF value for the concrete stayed constant, while the support fluid’s type and MF were varied. Firstly, the viscosity of bentonite slurry was lowered to assess the impact of this change on the decrease in mattressing. Secondly, the experiment with the polymer slurry of substantially higher MF was carried out.

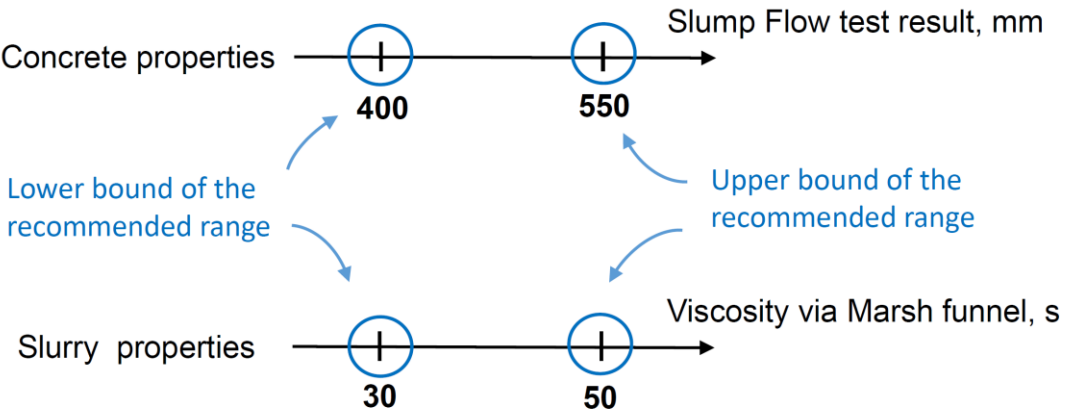


Figure 7.1. Recommended range of materials parameters for tremie placement method

The sequence of experiments and measured characteristics of materials are given in Table 7.1.

No experiment	Slurry MF, s	Concrete SF, mm
1	50 (bentonite)	560
2	48 (bentonite)	390
3	50 (bentonite)	465
4	35 (bentonite)	465
5	81 (polymer)	475

Table 7.1. Plan of experiments

## **7.2. Results of experiments**

### **7.2.1. Experiments 1 - 4: bentonite slurry.**

Step-by-step images of the concrete flow in experiments 1 – 4 are given in Figures 7.2-7.5. The time shown on shots is the time passed from the moment the concrete started escaping the tremie pipe. The following comments could be made regarding the observed results:

Experiment 1. The concrete escapes the pipe with no difficulties. The concrete was flowing around the reinforcement with a small difference in height between the central zone and cover zone. There were no signs of matting.

Experiment 2. The concrete could not flow out of the pipe. Shaking of the pipe was required to initiate the movement of the concrete. The concrete flow was limited to the centre of the pile and did not reach the reinforcement. There was no vertical flow of concrete: only downwards and side flow. Therefore, there was no displacement of the support fluid; hence, the process was not, in fact, the process of concrete placement by tremie method.

Experiment 3. The concrete was flowing out of the pipe with no difficulties. The concrete flow around the reinforcement did not close in the cover zone; it was leaving cavities filled with the support slurry. Visible matting formed with open channels through the whole thickness of the cover zone.

Experiment 4. The flow pattern was similar to the one obtained in experiment 1. The matting did not form when the concrete was flowing around the reinforcement. However, the formation of hidden cavities in a cover zone filled with support slurry and the slurry-concrete mix was possible.

There was an asymmetrical filling of the right and left sides of the gravity flow box in some experiments due to a slight tilt of the tremie pipe from the vertical axis. However, this did not affect the principal pattern of flow around the reinforcement and the extent of matting.

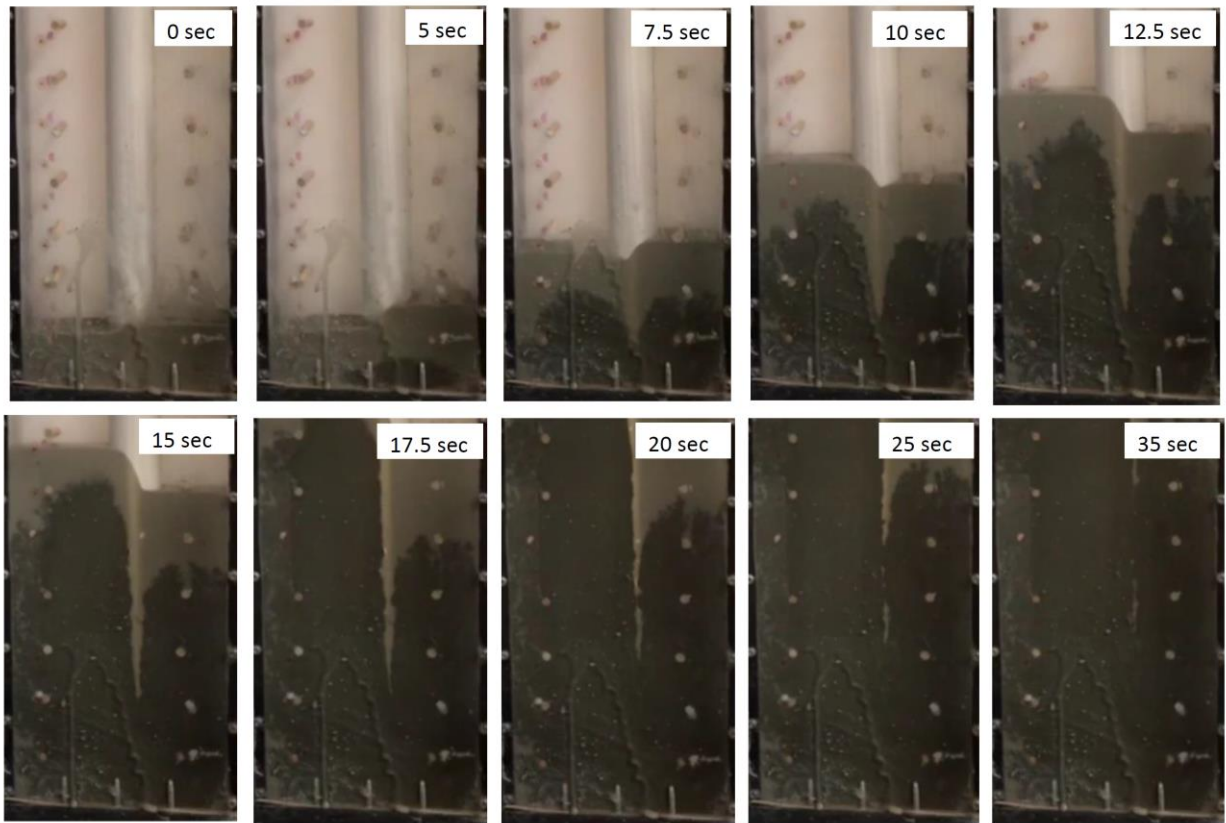


Figure 7.2. Flow Pattern for Experiment 1

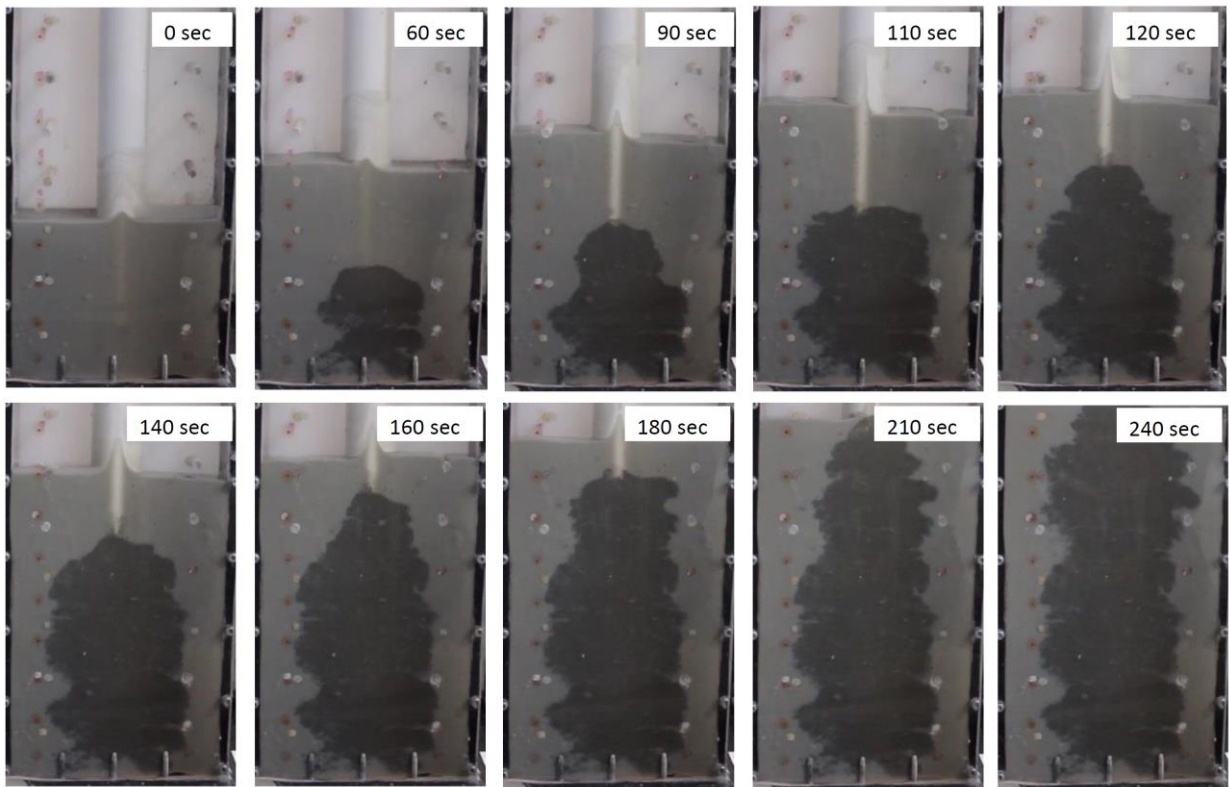


Figure 7.3. Flow Pattern for Experiment 2

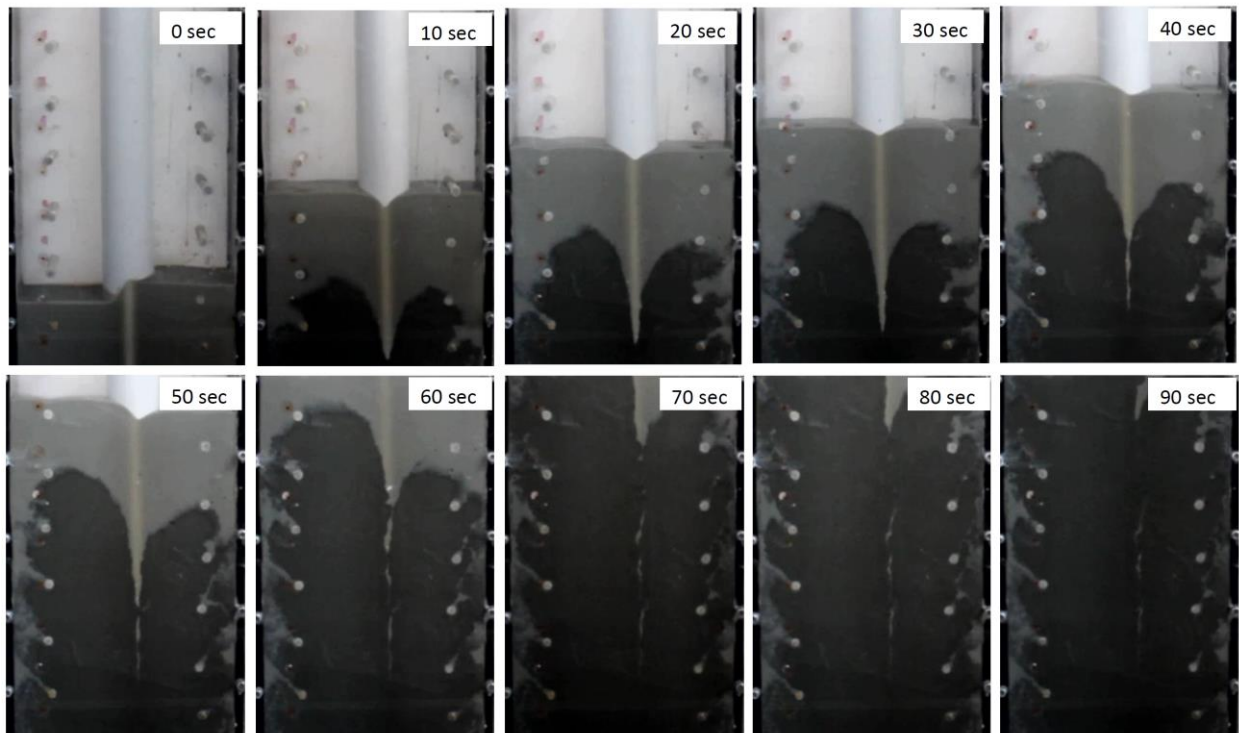


Figure 7.4. Flow Pattern for Experiment 3

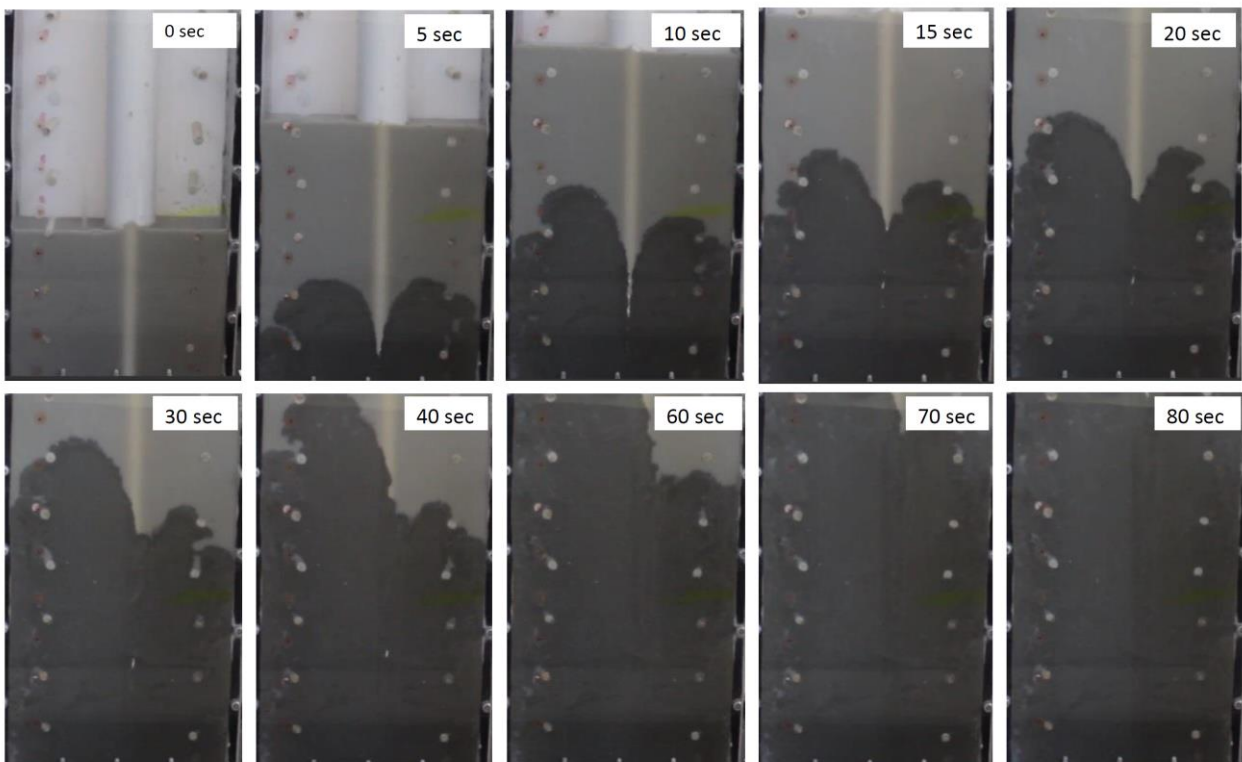


Figure 7.5. Flow Pattern for Experiment 4

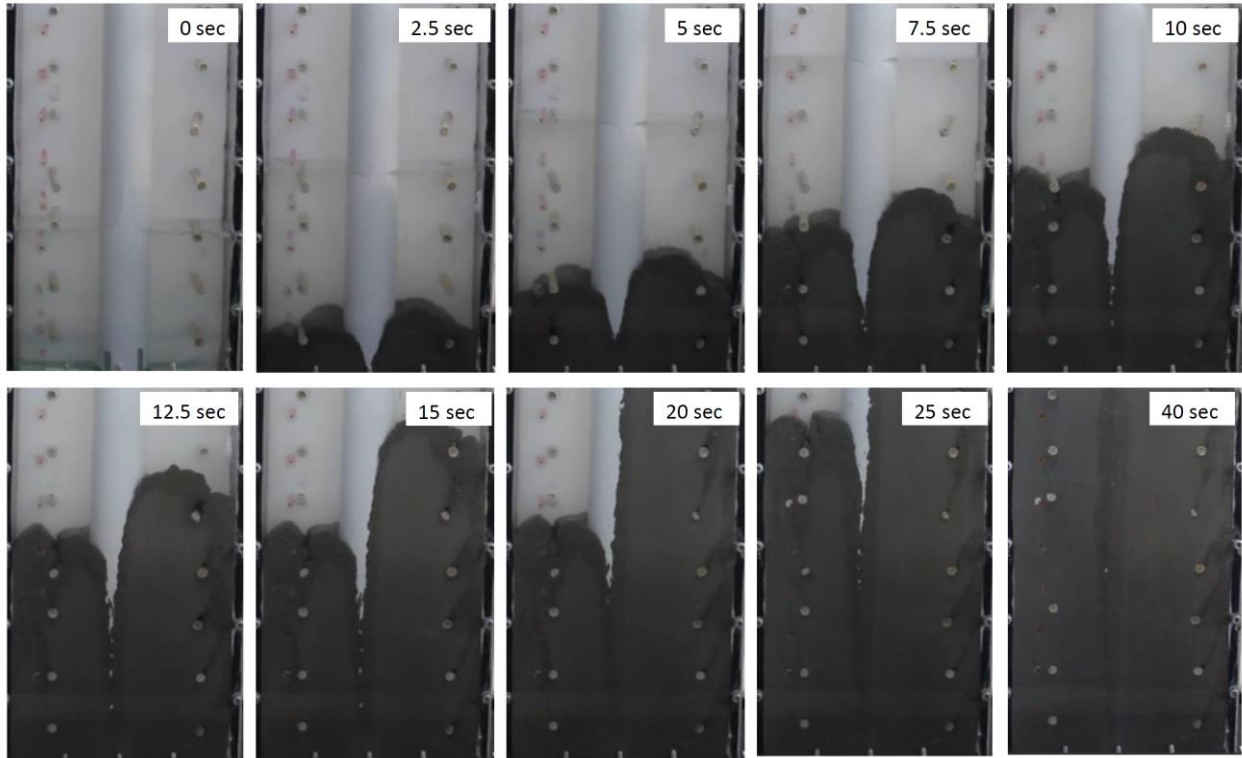


Figure 7.6. Flow Pattern for Experiment 5

### 7.2.2. Experiment 5: polymer slurry

Step-by-step images of the concrete flow are given in Figure 7.6.

The observed nature of filling the gravity flow box with concrete when polymer slurry is used differs significantly from the experiments where bentonite slurry was present. Concrete was filling the bottom of the box with no difficulties and then was uniformly working its way up. The speed of filling was higher than in previous experiments. Mattressing was absent.

## 8. Discussion

### 8.1. Zone of matting formation

The comparison of the final stages of concrete pour for all experiments is shown in Figure 8.1. These images were classified based on the presence/absence of matting. Then the field of varying parameters could be plotted, and the results marked on it (Figure 8.2).

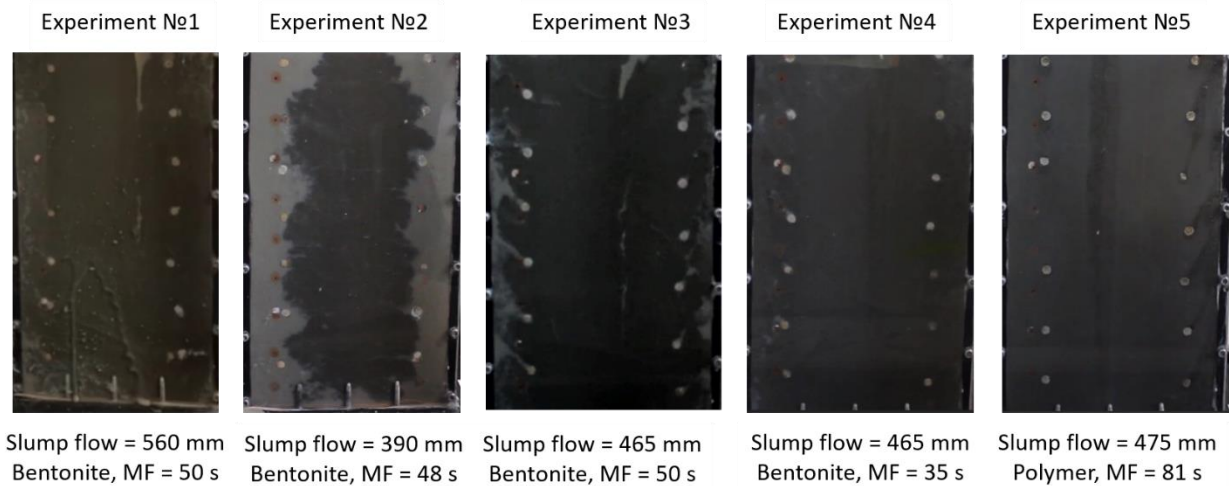


Figure 8.1. Final stage of pour images

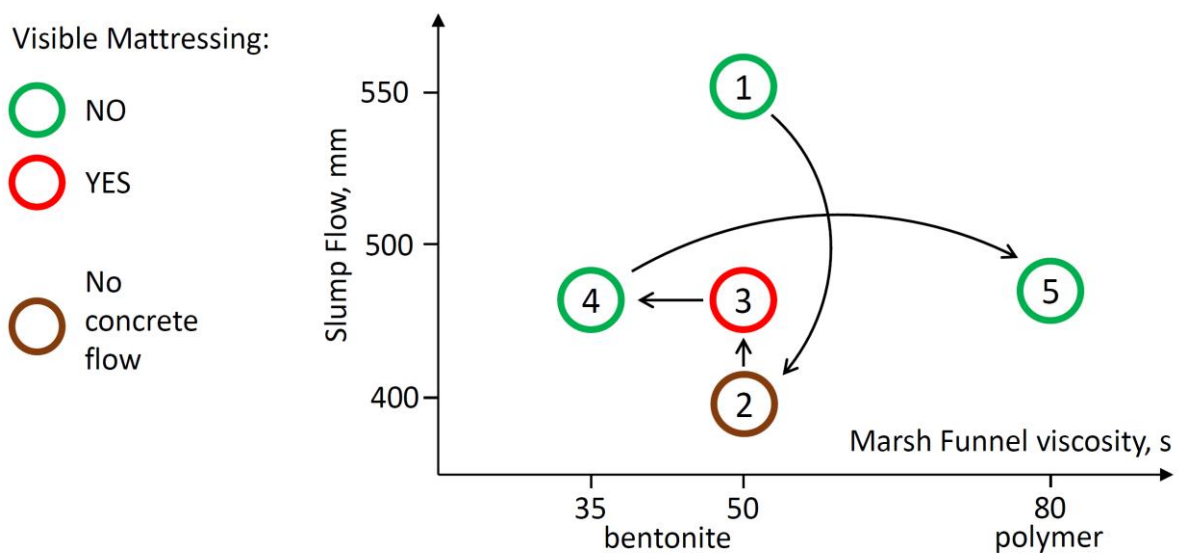


Figure 8.2. Results marked on the field of varying parameters

In accordance with the formulated hypothesis, yield stress is the primary influence on the risk of mattressing. Yield stress is the measure of fluid resistance to flow initiation. Its values for support fluids were obtained from rheometer tests; values of yield stress for concrete could be taken from the correlation (given in Kraenkel and Gehlen, 2018) between the Slump Flow test and Yield Stress (see Table 8.1)

Properties	Experiment				
	1	2	3	4	5
<u>Concrete</u>					
Slump Flow, mm	560	390	465	465	475
Yield Stress, Pa	66	222	123	123	115
<u>Support fluids</u>					
Marsh Funnel viscosity, s	50	48	50	35	81
Yield Stress, Pa	7,7	7,7	7,7	1,1	≈ 0

Table 8.1. Yield Stress values for concrete and support fluids

By knowing the yield stress values for concrete and support fluids, the results could be re-plotted in yield stress coordinates (Figure 8.3).

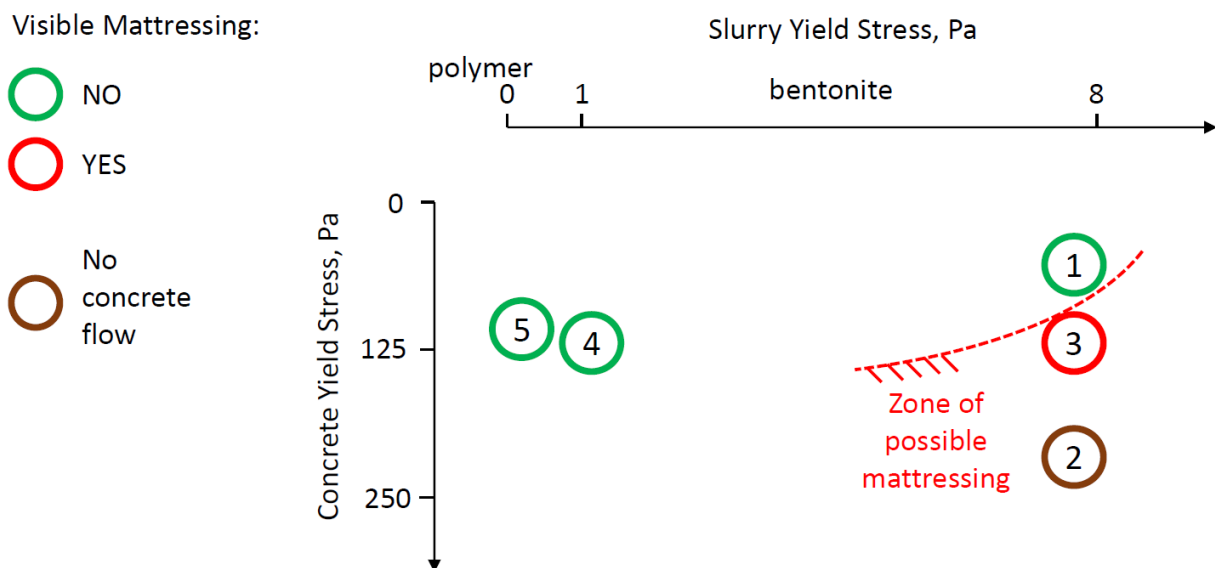


Figure 8.3. Results marked on the field of varying parameters in Yield Stress coordinates

The obtained diagram illustrates the connection between the location of the point in concrete yield stress/slurry yield stress coordinates and the formation of mattressing. Moreover, such interpretation of the results allows marking the zone of parameter combination where the mattressing is expected with high probability. A portion of this zone lies within the range, which is currently recommended by specifications for the

tremie method. Therefore, the results raise a question about the suitability of the bounds of the recommended ranges with respect to the risk of matting.

### 8.2. Comparison of flow patterns

In the literature review it was noted that the researchers mainly focus on the influence of reinforcement spacing on the flow pattern. The influence of the characteristics of the support fluid on the flow pattern for the fixed reinforcement parameters is less researched.

Video recordings allow to analyse step-by-step the flow patterns with slurries of varying characteristics. Such analysis was conducted based on the comparison between the pairs of the flow pattern images for the cases of slurries with the different material composition (bentonite and polymer slurry). The comparison was also conducted for the cases of slurries with the same material composition (bentonite) but with variation in characteristics to such an extent that it influences the matting formation.

A programming software for image processing was used for the analysis. The splitting of video files into video fragments and the creation of the appropriate sequence of images from them (storyboard) was carried out with the program Movavi Video Editor (Movavi, 2019). Further image processing was carried out with Photoshop program (Adobe, 2018). Photoshop allows getting a black and white version of the image by dividing the image into black and white areas based on the variation of brightness of the initial image (Figure 8.4). Additionally, the boundary between zones filled with concrete and support fluid could be identified, which helps to create a picture of step by step spread of the flow boundary.

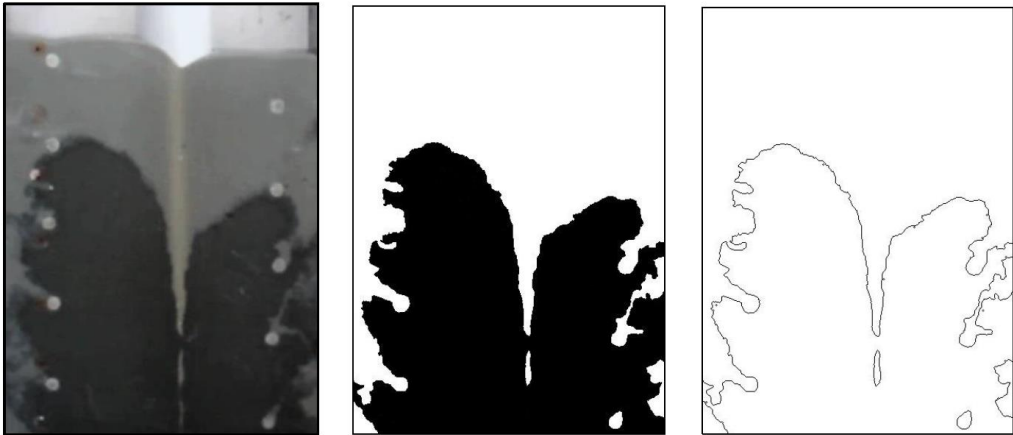


Figure 8.4. The sequence of image processing

### **8.2.1. Bentonite and polymer slurry**

The flow patterns of concrete in experiment 4 (bentonite slurry) and experiment 5 (polymer slurry) were compared (see Figures 7.5 and 7.6). The measured values of Viscosity via Marsh Funnel for bentonite and polymer slurry were 35 and 81 sec respectively. There was no mattressing in either experiment, but the pattern of flow around the reinforcement had notable differences.

The concrete in the experiment with bentonite slurry flows around reinforcement stick in two directions – from the side and from above - with approximately the same intensity. The flow pattern agrees with the one described in the literature: there is a difference between the level of concrete in the central zone and the cover zone. The portion of concrete contained in this volume is flowing above the reinforcement. The flow around reinforcement from the side is provided by the horizontal component of the flow, which is complemented by the concrete moving upwards in the cover zone along the side wall of the gravity flow box.

The flow pattern of the concrete for the case of polymer slurry is closer to the case for the concrete pour without reinforcement described in the literature. There is practically no difference between the level of concrete in the central zone and cover zone. The horizontal component of the flow is absent, and the concrete is filling the box by rising upwards. Due to the vertical movement, the concrete is coming from left and right of reinforcement by uniform flows, which meet at the top of the stick. Thus, no cavities promoting mattressing were left behind. The visual pattern of the flow does not show any signs of resistance to concrete flow from the polymer slurry. Polymer yield stress values are close to zero; therefore, there is no resistance to concrete flow. This confirms the hypothesis about the significance of support fluid's yield stress in terms of its influence on the flow pattern throughout the process of tremie concrete placement.

Rheometer tests have shown that the polymer slurry has yield stress close to zero for a wide range of Marsh Funnel viscosity values (the tests were carried out for the fluids with Marsh Funnel viscosity of 81 s and 159 s). Based on the hypothesis about the decisive impact of support fluid's yield stress, it could be concluded that the use of polymer slurry as the support fluid gives a substantially lower probability of mattressing than the use of bentonite slurry (given other things being equal and, most importantly, assuming the same characteristics of concrete). It is recommended to do the additional comparative series of experiments with bentonite and polymer to obtain reliable evidence to confirm

this hypothesis. However, based on the results, it could be stated that in the situation when there is a need to provide guaranteed protection against matting and the use of polymer slurry is not restricted, then the replacement of bentonite with polymer is a solution.

**8.2.2. Bentonite slurry: cases where matting is and is not present**

Since the bentonite slurry as a support fluid is currently used more frequently, then the study of cases where matting was formed at the displacement of bentonite slurry by the concrete is more important for now.

In this regard, a comparison between the flow patterns for experiment 3 (matting is present) and experiment 4 (matting is not present) was conducted. Concrete of the same characteristics was used in both experiments. Only the characteristics of the bentonite slurry used as the support fluid differed. The results of the contrasting processing of the left half of the images (Figure 8.5) in comparable stages of flow will be used for clarity.

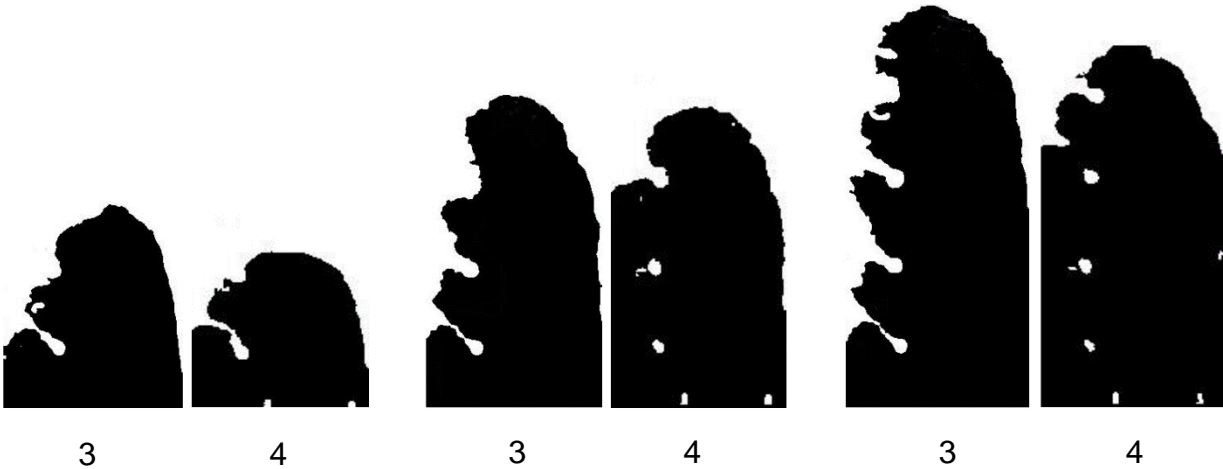


Figure 8.5. Comparison of flow patterns for experiments 3 and 4

The initial stage of filling the bottom area of gravity flow box and flowing around the bottom layer of reinforcement does not show significant differences: an open cavity in a cover zone is formed at the beginning in both cases. However, the flow pattern that follows is different: concrete is filling the cavities located behind the reinforcement in the cover zone in experiment 4 and matting does not form. Cavities in experiment 3 stay open, the concrete does not reach the side wall of the gravity flow box in the cover zone and hence pronounced matting is forming.

The detailed picture of flow around reinforcement should be studied to understand the differences in the process of filling the cover zone located behind the reinforcement. The 50x50 mm area around the third reinforcement stick was chosen for comparison in both cases (Figure 8.6). Consecutive pictures of flow around the reinforcement stick are shown in Figures 8.7 and 8.8.

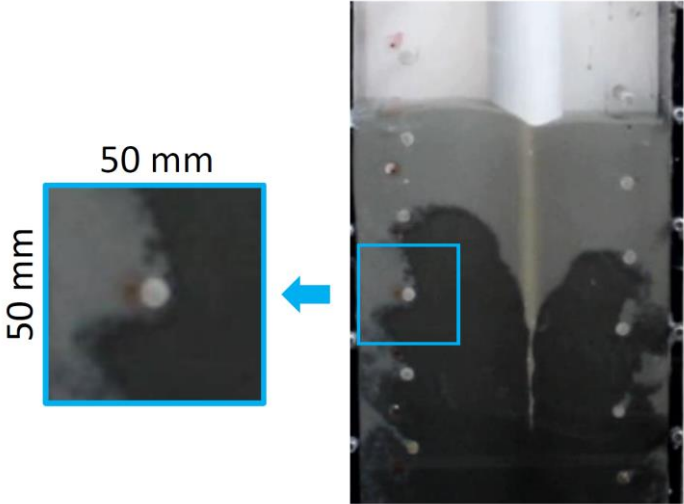


Figure 8.6. Cut-out fragment for assessment of flow pattern around reinforcement

The comparison of flow patterns has identified the following main differences. The ratio of the vertical component of flow velocity (along tremie pipe) to horizontal component (perpendicular to tremie pipe) in experiment 3 is noticeably higher than in experiment 4 (from Figures 8.7 and 8.8). More concrete rises along the tremie pipe and streams around the reinforcement at a greater distance from the reinforcement than in experiment 4. Top and bottom parts of the flow envelope are visually more uniform in experiment 4; the reinforcement is “wrapped” more tightly in the direct contact zone. In comparison with experiment 3, the lower part of the flow is fueled by additional concrete flow rising from the bottom along the side wall of the gravity flow box which allows to eventually overcome the resistance of the support fluid and displace it from the area around the reinforcement.

Why there is such a difference in concrete flow pattern, which leads to matting in experiment 3? Since these two comparable processes only differ in the properties of the bentonite slurry, then the cause of differences in flow patterns should be sought in the influence of the support fluid characteristics.



Figure 8.7. "Enveloping" of reinforcement in Experiment 3

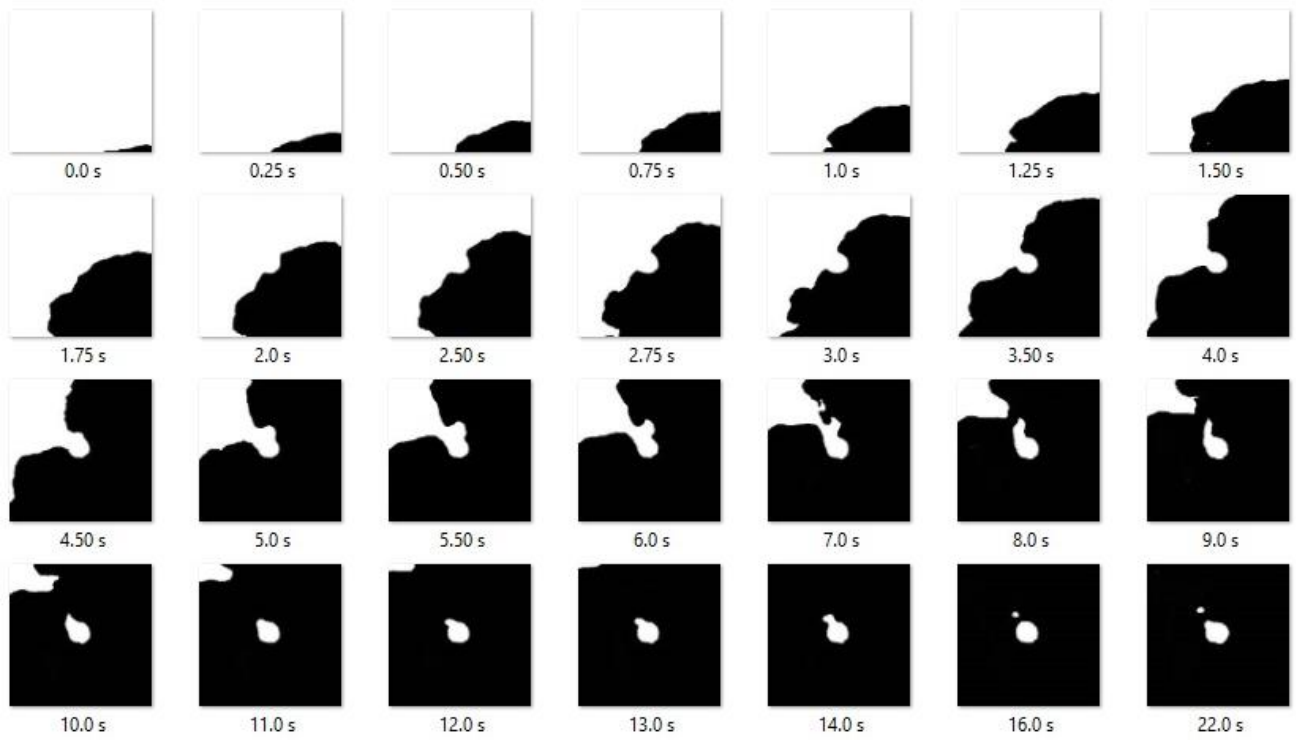


Figure 8.8. "Enveloping" of reinforcement in Experiment 4

Consider the process of gradual spreading of the concrete flow into the support fluid when “enveloping” the reinforcement, which results in the formation of the cavity. Outer boundaries of the concrete flow for the consecutive time intervals from 0 to 40 seconds starting from the inflow of concrete in the shot (obtained from the image processing for experiment 3) were combined in Figure 8.9 (numbers are time in seconds).

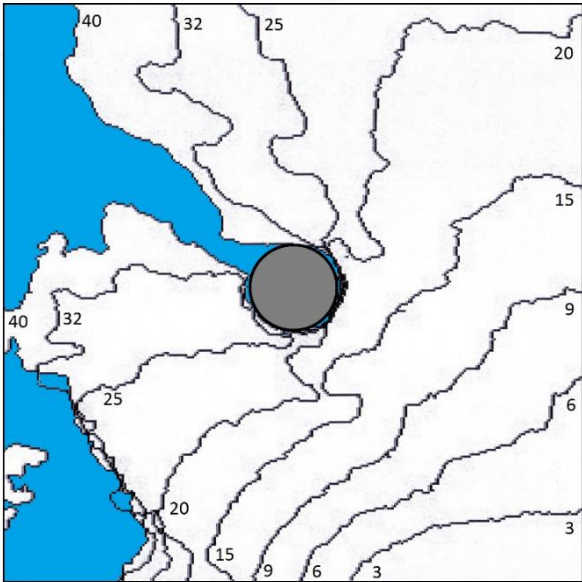


Figure 8.9. Stages of “enveloping” at matressing formation

The zone of slurry in a cavity, which was not eventually filled by concrete, is marked in blue. As it was mentioned earlier, the distinctive feature of this pattern is a higher ratio of vertical to horizontal components of concrete flow velocity in comparison with the case where matressing does not form. The quantitative assessment of the ratio of vertical to horizontal component of velocity for the upper right and lower left parts of flow at the moment of contact with reinforcement could be done. Figure 8.10 shows the location of the outer boundary of the flow for several consecutive time intervals from the moment of contact with reinforcement. Vertical and horizontal displacements of the boundary are also marked there. The ratio of vertical displacement of the upper right part of the flow to horizontal displacement of the lower left part of the flow is given below:

For experiment 3 (matressing is present):  $11/3.7 = 3.0$

For experiment 4 (matressing is absent):  $7.1/3.6 = 2.0$

The difference in flow velocity ratio for experiments 3 and 4 is  $3.0/2.0 = 1.5$ .

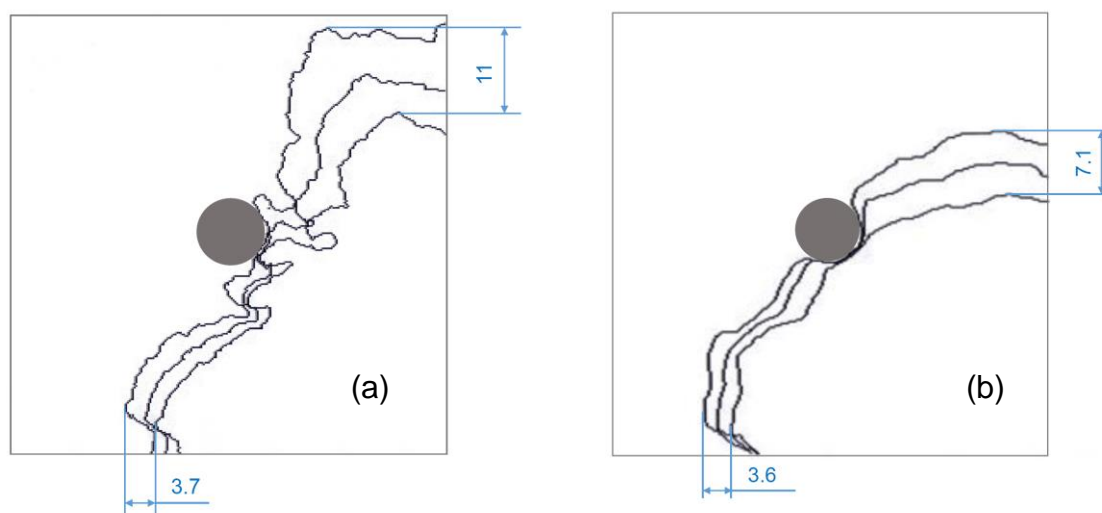


Figure 8.10. Displacement of concrete boundary in experiment 3 (a) and 4 (b)

The results indicate higher slurry resistance to the concrete horizontal flow in experiment 3 (mattressing is present) and, thus, there is greater resistance to filling the cover zone than in experiment 4. This result could be compared to the differences in the slurry characteristics. The rheometer tests of the support fluids gave the following results: bentonite slurry with yield stress 7.7 Pa and 1.1 Pa was used in experiments 3 and 4 respectively. The higher yield stress of slurry results in the higher resistance to the displacement of the slurry located in between the side wall and progressing horizontal concrete flow. Therefore, the stronger the resistance experienced by the concrete flow to horizontal displacement when entering the cover zone, the higher the redistribution of this flow towards the vertical direction within the pile core, which increases the probability of mattressing.

This suggestion was additionally checked by the numerical analysis, details of which are described in the next section.

## 9. Numerical analysis

As it was noted in the literature review, numerical modelling is an effective way to study the processes of concrete flow. Modelling allows identifying the relationship between physicommechanical properties of the support fluid and the flow parameters. However, methods for the numeral modelling of multi-fluid flows are complicated, insufficiently

developed for the simultaneous interaction of several fluids and rigid bodies and require careful validation with experimental data.

Therefore, a fully developed numerical modelling of flow cannot be completed within the scope of this project. However, it is possible to substantially simplify the problem statement for modelling since only a qualitative assessment is required in this case. Hence, numeral modelling could be used to qualitatively prove that the higher yield stress of slurry results in the higher redistribution of the flow towards the vertical direction within the pile core, which increases the probability of matting.

Only the distribution of displacements in concrete and support fluid at the moment of contact between the concrete and reinforcement will be studied. It will be done by analogy with plots in Figure 8.10. The area of modelling will also be restricted to 50x50 mm square, in the centre of which the cross-section of the “enveloped” reinforcement is located (Figure 9.1). The initial position of the boundary separating concrete and slurry is assumed to be represented by an arc of a circle which touches the surface of the reinforcement.

Secondly, the loading will be represented as a radial pressure distributed along the arc at the corner of the concrete segment. It will be assumed that such loading reflects the action of the concrete coming from the tremie pipe.

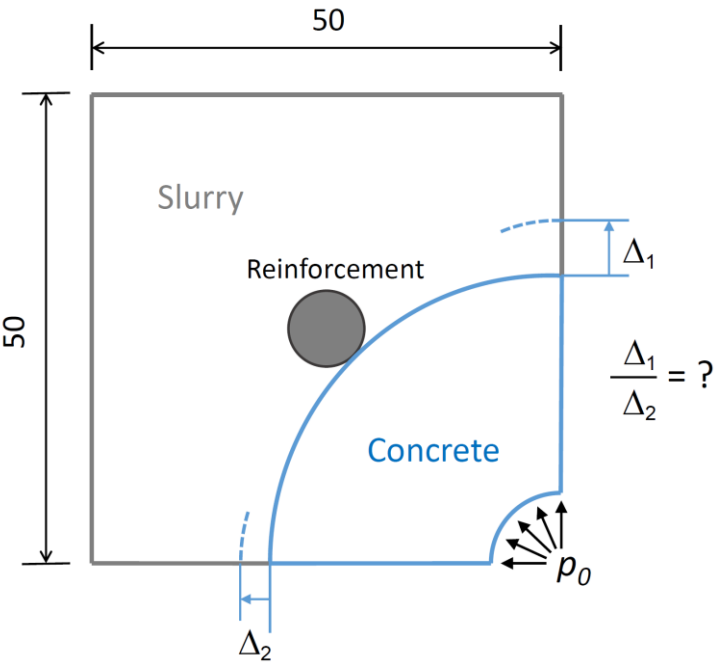


Figure 9.1. Schematic of model geometry

Thirdly, since the concrete and support fluid shear rates are small during the tremie concrete placement process (Lam and Jefferis, 2014), the influence of flow velocity on the shear stress is negligible. It will be assumed that the main characteristic of the fluid which influences the displacement distribution is yield stress. Therefore, it is possible to move from the Bingham plastic model to an elasto-plastic model. Characteristics of the elasto-plastic behaviour of the bentonite slurry can be obtained from its rheometer test results. The “shear stress – shear angle” graph could be plotted for the initial stage of fluid loading, and then the point of transition from elastic state to plastic yield could be found.

It is worth noting that the aim here is not to compare calculated and experimental displacements  $\Delta_1$  and  $\Delta_2$ . Instead, the qualitative relationship between the ratio  $\Delta_1/\Delta_2$  and the yield stress of the support fluid at the fixed value of the concrete yield stress needs to be determined.

Given the above simplifications, the program RFEM by Dlubal Software was used for the non-linear finite element analysis of the elasto-plastic behaviour of several bodies in contact. The choice of software was determined, firstly, by its capabilities and practical focus on structural analysis in the context of civil engineering. Secondly, plenty of webinars for the quick mastering of the program are available on the developer’s website. In addition, the developer is giving 90-days free trial license for all program modules.

The following actions were performed for the numerical analysis. Firstly, the geometrical model consisting of two bodies (concrete and slurry) was built (Figure 9.2). Although the flow process is, in fact, plane (2D), the geometrical model was built in 3D since the program only works with 3D objects. The model’s dimensions were matched with the ones given on the diagram in Figure 9.1. The thickness of the bodies was taken as 10 mm. Based on the geometrical model, an FE-model was built, and boundary conditions were applied (Figure 9.3). The thickness of the bodies was kept constant throughout the loading, thus maintaining plane strain conditions.

The reinforcement was not included in the model as a separate body. A support was introduced in the model (Figure 9.4) to model an obstacle to concrete flow created by reinforcement at the moment of contact between concrete and reinforcement. The support allowed to impose restrictions on the displacement of concrete and slurry at the point of contact with reinforcement. The introduction of the support resulted in all the displacements at this point being equal to zero at the given moment in time.

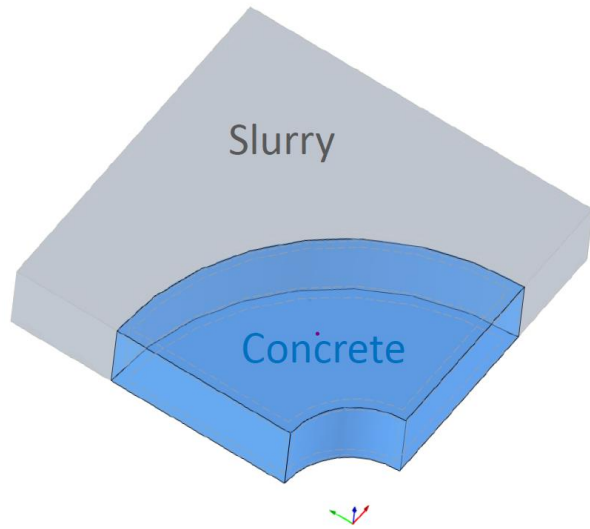
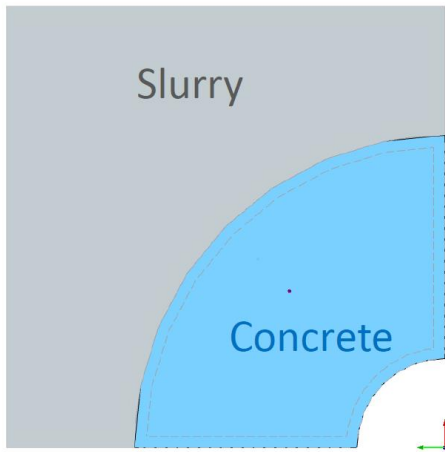


Figure 9.2. 3D model for concrete and slurry

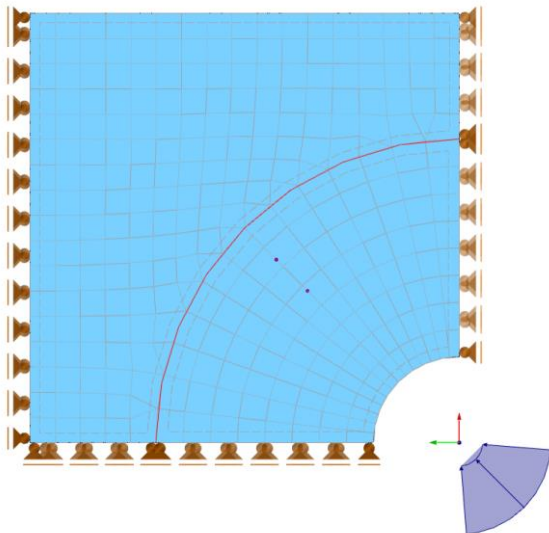


Figure 9.3. FE-model

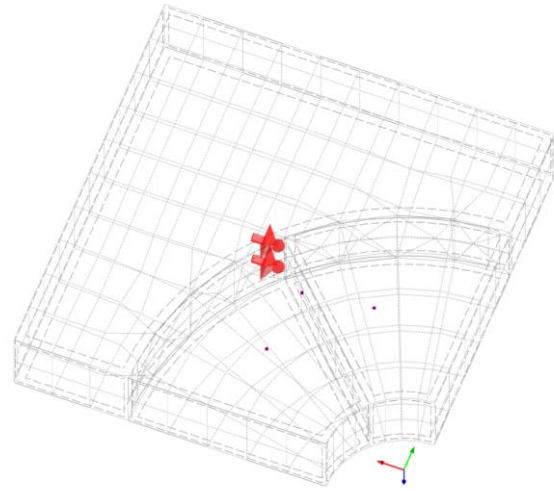


Figure 9.4. Support at the point of contact with reinforcement

The loading was applied in the form of uniformly distributed pressure in accordance with the diagram in Figure 9.1.

The elasto-plastic model parameters for the bentonite slurry were taken from the rheometer tests (see Figure 9.5). Initial angular movement of the rheometer rotor occurs through elastic deformation of slurry to the point of yield stress at which the gradient of the shear stress changes and the rotational speed of the rotor starts to increase.

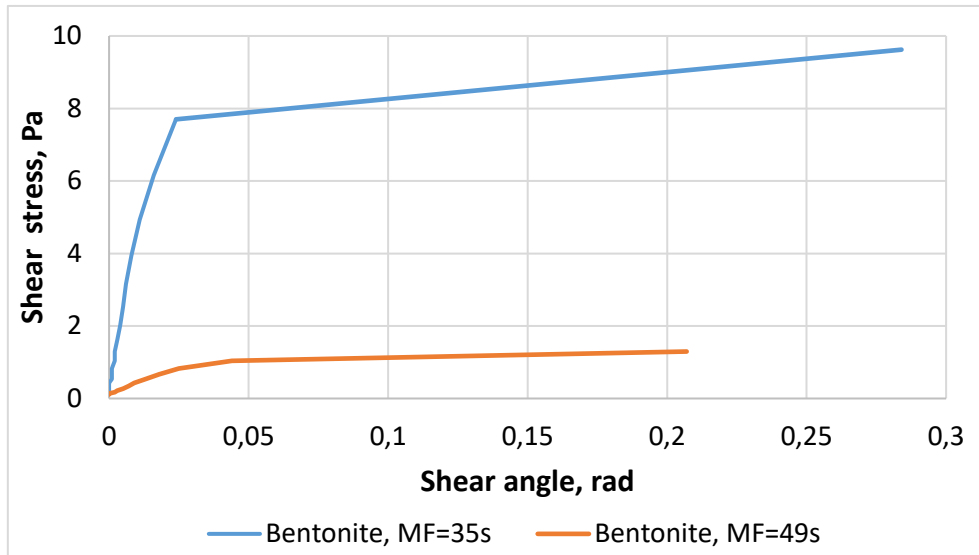


Figure 9.5. Elasto-plastic characteristics of bentonite

Yield stress and shear modulus were obtained from the Figures 6.4 and 9.5 respectively. The value of Poisson's ratio was taken close to 0.5, which is typical for incompressible fluid.

Since the rheological characteristics of concrete were not measured directly, the concrete yield stress was calculated from the literature data (Kraenkel and Gehlen, 2018) for correlations between Slump Flow (SF) and Yield stress (YS):

$$YS = 10^{11} \cdot SF^{-3.34} = 10^{11} \cdot 465^{-3.34} = 123 \text{ Pa}$$

Table 9.1 shows the characteristics of materials used for calculations. Two cases were analysed differing only by characteristics of bentonite slurry. Self-weight of fluids was not considered.

The nonlinear calculations were performed by the large deformation method with rebuilding of the stiffness matrix after each load increment.

Distribution of deformations in concrete and slurry under the action of 1 kPa load for two calculation cases are given in Figure 9.6. Calculations for case A gave more pronounced vertical displacements. This can be confirmed by looking at the concrete boundary displacement (see Figure 9.7).

Material	Properties	Calculation cases	
		A	B
Bentonite Slurry	Shear modulus, Pa	321	23.6
	Poisson's ratio	0.499	0.499
	Yield stress, Pa	7.7	1.1
Concrete	Shear modulus, Pa	2500	same
	Poisson's ratio	0.499	same
	Yield stress, Pa	123	same
Comments		Experiment 3, MF=50 s mattressing present	Experiment 4, MF=35 s no mattressing

Table 9.1. Characteristics of material for numerical modelling

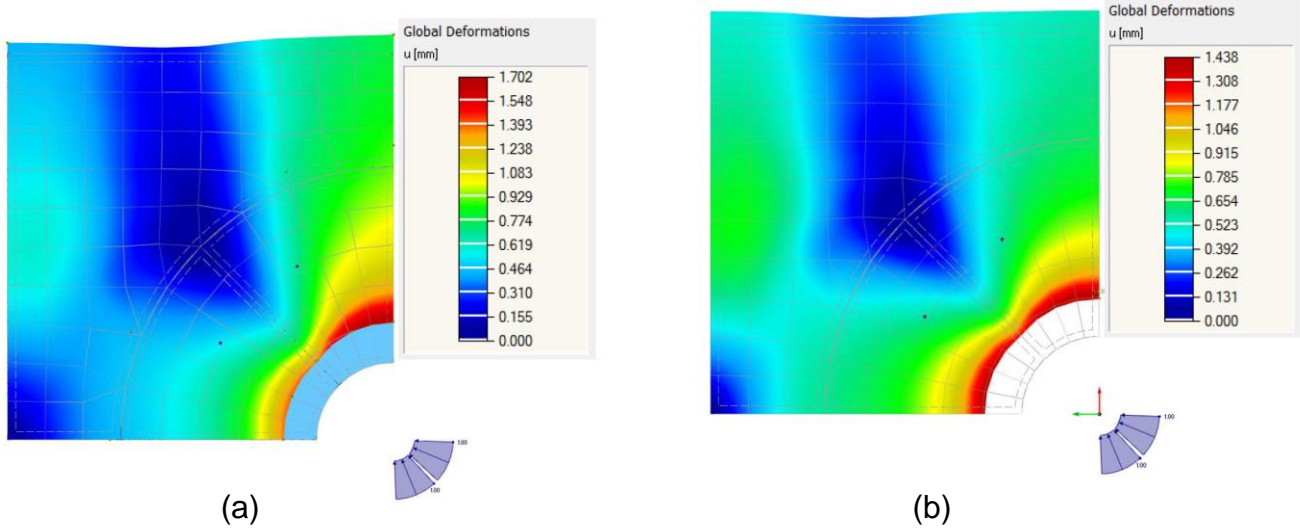


Figure 9.6. Displacement distribution for Case A (a) and Case B (b)

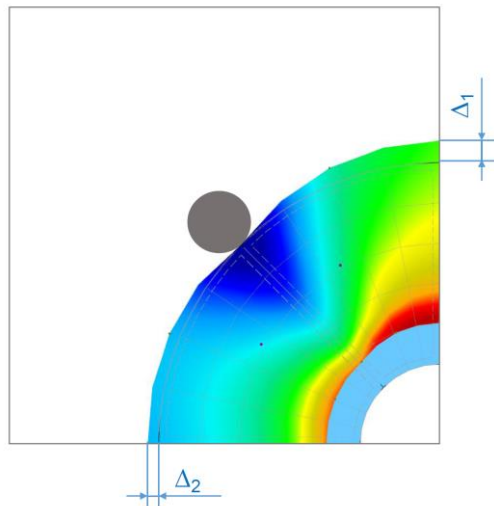


Figure 9.7. Displacement of concrete at boundary

Ratio  $\Delta_1/\Delta_2$  for case A (Experiment No 3) is equal to:

$$\Delta_1/\Delta_2 = 0.887/0.439 = 2.0,$$

Ratio  $\Delta_1/\Delta_2$  for case B (Experiment No 4) is equal to:

$$\Delta_1/\Delta_2 = 0.624/0.566 = 1.1$$

The difference in values of ratio  $\Delta_1/\Delta_2$  between calculation cases A and B is equal to  $2.0/1.1 = 1.8$ . The value obtained after processing of the video recordings of the experiments was 1.5, which is comparable to 1.8 considering all the adopted simplifications. Therefore, this supports the hypothesis that the ratio  $\Delta_1/\Delta_2$  is determined by the value of yield stress of the slurry compressed in the cover zone.

Figure 9.8 shows the picture of the development of the plastic zone in the slurry obtained from the modelling results. The development of the plastic zone starts specifically from the compressed slurry in the cover zone. The higher the slurry yield stress, the higher the resistance to the horizontal flow of concrete, and the more difficult it is to displace the slurry layer from the cover zone. Difficulty in displacing the slurry from the cover zone, in turn, leads to an increased probability of matting.

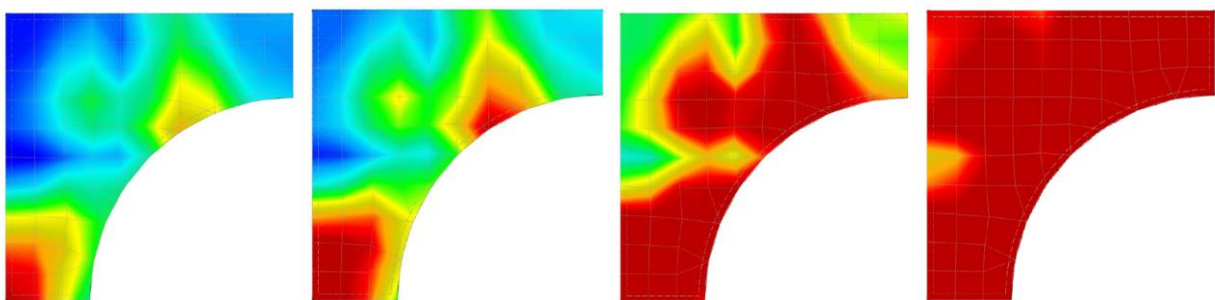


Figure 9.8. Development of plastic zone in slurry

## 10. Limitations of the research

Experiments were carried out by following the industrial guidance on the concrete placement by tremie method. Nevertheless, the results of this research should be interpreted with account for limitations determined by the laboratory conditions.

1. The process was modelled in reduced scale relative to the dimensions of the possible real structure. The width of the gravity flow box, the diameter of tremie pipe, the maximum size of aggregates in concrete mixture and diameter of reinforcement were all scaled. The size of the scaled cover zone exceeded the minimum value to allow better visualization of the process. The study of the influence of the ground depth was not conducted.
2. The two-dimensional flow was considered.
3. Only horizontal reinforcement was considered. The vertical distance between reinforcement sticks was assumed to be equal to the distance between gravity flow box walls (i.e. the “cell” of the reinforcement mesh was represented by horizontal reinforcement segments and gravity flow box walls).
4. Effects associated with the height of the slurry column were not considered.
5. Effects associated with the geometry and physical characteristics of the soil surface were not considered.

The stated limitations do not change the physics and main causes of matting formation; however, they might influence the quantitative relationships between parameters of the process in real industrial conditions.

## 11. Conclusion and recommendations

1. The combination of concrete and support fluid parameters leading to matting was determined based on series of experiments using a laboratory set-up, which is a scaled version of the real process of concrete placement by tremie method. These parameters (Slump Flow = 50 s, Marsh Funnel viscosity = 460 mm) lie within the range currently recommended by literature for the tremie method. Therefore, the results of this work could have a practical value in terms of correcting the boundaries of the recommended ranges accounting for the risk of matting.

2. The influence of changes in concrete and slurry parameters on the extent of mattressing was studied. The zone of parameters combination where the defect is expected with high probability was marked. It is advisable to conduct more tests in future research to define the boundary of mattressing zone with greater accuracy, considering the limited number of experiments in this project.
3. Based on the characteristics of the bentonite and polymer slurry obtained from rheometer tests, it was shown that the formation of mattressing depends on the shear stress of the support slurry at low shear rates. For this reason, the use of polymer slurry, the yield stress of which is close to zero for the wide range of Marsh Funnel viscosity values, substantially lowers the risk of mattressing.
4. The flow patterns around the reinforcement for the cases resulting in mattressing were compared to those for cases where mattressing was absent. The flow pattern of concrete in the case of polymer slurry is similar to the one described in the literature for the case of concrete flow when no reinforcement is present and is substantially different from the concrete flow pattern in the bentonite slurry. In turn, the difference in flow pattern around the reinforcement for bentonite slurry was determined by yield stress value. There is a correlation between slurry yield stress and the ratio between vertical and horizontal concrete flow at the moment of “enveloping” the reinforcement.
5. The influence of yield stress of slurry on the resistance to the concrete coming into the cover zone was confirmed by the numerical modelling. Modelling was conducted by non-linear finite element analysis adopting several simplifying assumptions in terms of physical parameters of the materials, the loading source and boundary conditions. This allowed obtaining results for a preliminary assessment. More detailed reproduction of the physical processes of concrete and slurry flows by numerical modelling accounting for more factors could be a promising direction of research and is recommended for use in future studies.

## References

Adobe Photoshop (2018). Available at [www.adobe.com](http://www.adobe.com)

AMETEK Brookfield viscometer (2017). *More solutions to sticky problems: A guide to getting more from your Brookfield Viscometer*. AMETEK Brookfield, Inc.

Asirvatham, J., Tejada-Martinez, A., Gray Mullins, G. (2017). *Numerical Modeling of Concrete Flow in Drilled Shaft*. Proceedings of the 2017 COMSOL Conference in Boston.

Barnes, H. A., and Walters K. (1985). The yield stress myth? *Rheologica Acta*, Vol. 24, No. 4

Bowen, J. (2013). *The Effects of Drilling Slurry on Reinforcement in Drilled Shaft Construction*. Graduate Theses and Dissertations. University of South Florida.

Brown, D. A., Turner, J. P., and Castelli, R. J. (2010). *Drilled shafts: Construction Procedures and LRFD Design Methods*. Publication No. FHWA NHI-10-016, Federal Highway Administration, U.S. Department of Transportation, Washington, D.C., 970 p.

BSI (2009). BS EN 12350-8:2009 *Testing fresh concrete: Slump Flow Test*. British Standards Institution.

Buglass, D. (2018). *Flow of Tremie Concrete in Deep Foundations*. Master's Final Report. Department of Engineering. University of Cambridge

Damji, A. (2018). *Degradation of Synthetic Polymer Support Fluids in Construction*. Master's Final Report. Department of Engineering. University of Cambridge.

Drilled shafts (2010). *Drilled Shafts: Construction Procedures and LRFD Design Methods*. Chapter 7. U.S. Department of Transportation. Federal Highway Administration.

EFFC/DFI (2018). *EFFC/DFI Best Practice Guide to Tremie Concrete for Deep Foundations* (2018). European Federation of Foundations Contractors and Deep Foundations Institute Concrete Task Group, 2nd edition.

Fédération internationale du béton fib (2006). *Model Code for Service Life Design*. Lausanne, Switzerland.

Fierenkothen, C. and Pulsfort, M. (2018). *The spreading of fresh concrete in bored piles—results of large and small scale model tests and numerical simulations*. Proceedings of the 19th International Conference on Soil Mechanics and Geotechnical Engineering, Seoul.

Kraenkel, T. and Gehlen, C. (2018). *Rheology and Workability Testing of Deep Foundation Concrete in Europe and the US*. Research Report No. 20-F-0107, Chair of Materials Science and Testing, Centre for Building Materials, Technical University of Munich

Lam, C., and Jefferis, S. A. (2014). *Interpretation of viscometer test results for polymer support fluids*. Proc., Sessions of GeoShanghai 2014 Int. Conf., GSP 242, ASCE, Reston, VA, 439–449.

Lam, C., Jefferis, S.A., Suckling, T.P., Troughton, V.M. (2015) *Effects of polymer and bentonite support fluids on the performance of bored piles*. Geotechnique.

Leutert (2015). Marsh Funnel: Product information. Available at <https://www.leutert.com>

Lubach, A. (2010). *Bentonite cavities in diaphragm walls. Case studies, process decomposition, scenario analysis and laboratory experiments*. Delft University of Technology.

Movavi Video Editor 15 (2019). Movavi Software Limited. Available at [www.movavi.com](http://www.movavi.com).

Mullins, G., Ashmawy, A., Anderson, B., Deese, G., Garbin, E., Johnson, K., Lowry, S., Stokes, M., Wagner, R. V., Winters, D. (2005). *Factors affecting anomaly formation in drilled shafts – Final Report*. Florida Department of Transportation BC-353-19. University of South Florida.

RFEM 5 (2016). *Spatial Models Calculated According to Finite Element Method*. Program Description. Dlubal Software GmbH.

Roussel, N. et al (2016). *Numerical simulations of concrete flow: A benchmark comparison*. Technical University of Denmark

## **Appendix. Risk Assessment Retrospective.**

Personal safety and safety of others are particularly important in project work. Compliance with Health & Safety procedures minimises the risks associated with the execution of the experiments and tests.

The Hazard Assessment form was completed before the commencement of laboratory experiments for this project. It identified the potential electrical, mechanical and physical hazards as well as hazardous substances. These were discussed in detail in Risk Assessment and Control of Substances Hazardous to Health (COSHH) forms. No Health & Safety accidents were encountered throughout the project.

Almost all risks associated with the project could be prevented by wearing appropriate Personal Protective Equipment (PPE). The general PPE included eye protection, lab coat/overalls, gloves and safety boots with steel toe caps. The significant risks were associated with hazardous substances outlined in COSHH form: these included cement, superplasticiser and bentonite. The fine cement and bentonite powder could cause the respiratory issues, while wet concrete could cause eye irritation and intoxication from breathing in. Therefore, the respiratory mask was worn at all times when working with these substances.

The hazard that was not initially accounted for was vibration from hand concrete mixer: the mixing continued for longer than expected. Therefore, muscle pain was encountered after the experiment. However, there was no risk of potential health problems since the experiments were separated in time, and the mixing time did not exceed the maximum allowed time of working with vibration equipment per day.

Therefore, overall, the Health & Safety procedures were carefully followed, and all experiments completed in a safe manner. Occasionally, there were some inevitable muscle pains and headaches due to working long hours in closed space carrying heavy equipment, although every effort was undertaken to minimise those.

If the project were to be repeated, a more accurate risk assessment would probably be required to minimise further the risks stated above. An automatic concrete mixer could be used to avoid working with the vibrating equipment. Moreover, the experimental procedure could be improved in such a way to allow for breaks without overly compromising on efficiency.